Assessing Outcomes in Stratospheric Aerosol Injection Scenarios Shortly After Deployment

Daniel M. Hueholt[1], Elizabeth A. Barnes[1], James Wilson Hurrell[1], Jadwiga H. Richter[2], and Lantao Sun[1]

[1]Colorado State University
[2]National Center for Atmospheric Research (UCAR)

April 20, 2023

Abstract

Current global actions to reduce greenhouse gas emissions are very likely to be insufficient to meet the climate targets outlined under the Paris Agreement. This motivates research on possible methods for intervening in the Earth system to minimize climate risk while decarbonization efforts continue. One such hypothetical climate intervention is stratospheric aerosol injection (SAI), where reflective particles would be released into the stratosphere to cool the planet by reducing solar insolation. The climate response to SAI is not well understood, particularly on short-term time horizons frequently used by decision makers and planning practitioners to assess climate information. This knowledge gap limits informed discussion of SAI outside the scientific community. We demonstrate two framings to explore the climate response in the decade after SAI deployment in modeling experiments with parallel SAI and no-SAI simulations. The first framing, which we call a snapshot around deployment, displays change over time within the SAI scenarios and applies to the question "What happens before and after SAI is deployed in the model?" The second framing, the intervention impact, displays the difference between the SAI and no-SAI simulations, corresponding to the question "What is the impact of a given intervention relative to climate change with no intervention?" We apply these framings to annual mean 2-meter temperature, precipitation, and a precipitation extreme in the first two experiments to use large ensembles of Earth system models that comprehensively represent both the SAI injection process and climate response, and connect these results to implications for other climate variables.

Supporting Information for "Assessing Outcomes in Stratospheric Aerosol Injection Scenarios Shortly After Deployment"

Daniel M. Hueholt[1], Elizabeth A. Barnes [1], James W. Hurrell[1], Jadwiga H. Richter [2], Lantao Sun[1]

[1]Department of Atmospheric Science, Colorado State University, Fort Collins, CO, USA

[2]Climate and Global Dynamics Laboratory, National Center for Atmospheric Research, Boulder, CO, USA

Contents of this file

Introduction This document contains additional useful information accompanying "Assessing Outcomes in Stratospheric Aerosol Injection Scenarios Shortly After Deployment." Supporting Information Text S1 concerns robustness: here, we discuss the binomial test for statistical significance, and provide a detailed description of the algorithm to calculate robustness. Supporting Information Text S2 describes the archive of bonus annual mean 2m temperature, annual mean precipitation, and simple intensity index timeseries provided for all IPCC-defined regions (van Oldenborgh et al., 2013). Finally, Figures S1 to S6 are supporting figures referenced in the paper.

Text S1. Robustness Our thresholds for robustness fall outside the 90% confidence bounds of the distribution expected by chance: that is, when robustness is calculated on 10,000 pairs of random vectors of length 21 (mimicking GLENS) and 10 (mimicking ARISE) sampled from a uniform distribution (Monte Carlo approach). These thresholds can be formally mapped to statistical significance using a binomial test. As applied here, the binomial test null hypothesis is that a nearly-equal number of SAI and no-SAI members will exceed and subceed each other. The binomial test calculates the probability of a given number of successes by applying the binomial distribution, which has three parameters: the probability of the null q, the number of tests n, and the value of interest x (Equation 1). The probability of a given number of "successes" is the probability of obtaining any given value of robustness.

$$P(x) = \frac{n!}{x!(n-x)!} q^x (1-q)^{(n-x)} \tag{1}$$

q is the probability of the null. In the default binomial distribution, $q = 0.5$; for robustness, this is weighted by the choice of B to not be a fair "coin toss." Rather, $q = \frac{Z-B}{Z}$ where Z denotes the size of the ensemble. n is the number of ensemble members. Finally, x is the number of successes for which the probability is computed. Using the binomial test, the p-value can be calculated as $P(x \geq 15)$ with $q \approx 0.48$ and $n = 21$ for GLENS, and $P(x \geq 7)$ with $q = 0.4$ and $n = 10$ for ARISE. For GLENS, the threshold corresponds to a p-value of $p = 0.02$; for ARISE, $p = 0.05$. We had chosen a significance threshold of $p < 0.1$; thus, our robustness threshold corresponds to standard values of statistical significance. We prefer to discuss robustness in terms of the percent of the distribution expected by chance that the threshold falls outside. We believe this is the most intuitive way to understand the information that robustness conveys about the consistency of a response. The above discussion shows robustness satisfies statistical significance conventions, as well.

We now detail the algorithm to calculate robustness. In the code repository accompanying this work (Hueholt, 2022, doi.org/10.17605/OSF.IO/5A2ZF), robustness is implemented in the module `fun_robustness.py`.

1. Choose the time period of interest. We define this time period as (2025-2029) for GLENS and (2040-2044) for ARISE, corresponding to the time horizon of 10 years after SAI deployment which we focus on in our work.

2. The user defines the threshold value B. A given SAI member must exceed or subceed this number of no-SAI members to be counted as a robust signal. We set B equal to 11 for GLENS and 6 for ARISE given their differing ensemble sizes.

3. Choose a realization from the SAI ensemble.

4. Compare the mean value of the given SAI member during the time period to the mean values from the corresponding time period of every no-SAI member. Calculate the number of no-SAI realizations that the SAI member exceeds and subceeds. These two numbers are retained as G_{exceed} and $G_{subceed}$.

5. Repeat steps 3 and 4 for each SAI member. In this way, each SAI member will be compared to every no-SAI realization.

6. The number of SAI realizations surpassing B is summed for each of G_{exceed} and $G_{subceed}$ ensuring both negative- and positive-signed forced responses from SAI can be captured. Mathematically, this describes the calculation of $\left\{ \mathrm{n}\left(r_{S_{\theta,\phi r_z} > \overline{\tilde{S}_{\theta,\phi r_{\{B\}}}}} \right), \mathrm{n}\left(r_{S_{\theta,\phi r_z} < \overline{\tilde{S}_{\theta,\phi r_{\{B\}}}}} \right) \right\}, \Big| \forall z \in \{0, ..., Z\}$ in Equation 1 in Section 2.3 of the accompanying paper.

7. The maximum of the two numbers from the previous step is the robustness ρ at the given grid point and time period. If the robustness at a point is greater than or equal to 15 members (GLENS) or 7 members (ARISE), we consider the point to be "robust." These thresholds correspond to values that fall outside the 90% confidence bounds of the distribution expected by chance, i.e. when this calculation is completed for 10,000 pairs of vectors randomly sampled from a uniform distribution.

8. The calculation is repeated for every grid point to generate a map of robustness.

Text S2. Archive of Timeseries. In order to comprehensively illustrate the regional climate response in GLENS and ARISE, we provide timeseries for annual 2m temperature, annual precipitation, and the simple intensity index at all IPCC WG1-AR5 regions. These figures are located at the following archive: doi.org/10.17605/OSF.IO/5A2ZF. This archive also contains the code and data necessary for reproducing the figures and results discussed in the paper.

References

Hueholt, D. (2022). *PAPER - Assessing Outcomes in Stratospheric Aerosol Injection Scenarios Shortly After Deployment.* Retrieved 2022-12-16, from `https://osf.io/5a2zf/` (Publisher: OSF)

van Oldenborgh, G. J., Collins, M., Arblaster, J., Christensen, J. H., Marotzke, J., Power, S. B., ... Zhou, T. (2013). Annex I: Atlas of Global and Regional Climate Projections. In T. F. Stocker et al. (Eds.), (pp. 1311–1393). Cambridge, United Kingdom: Cambridge University Press. Retrieved 2022-05-19, from `https://www.ipcc.ch/report/ar5/wg1/` (Num Pages: 84)

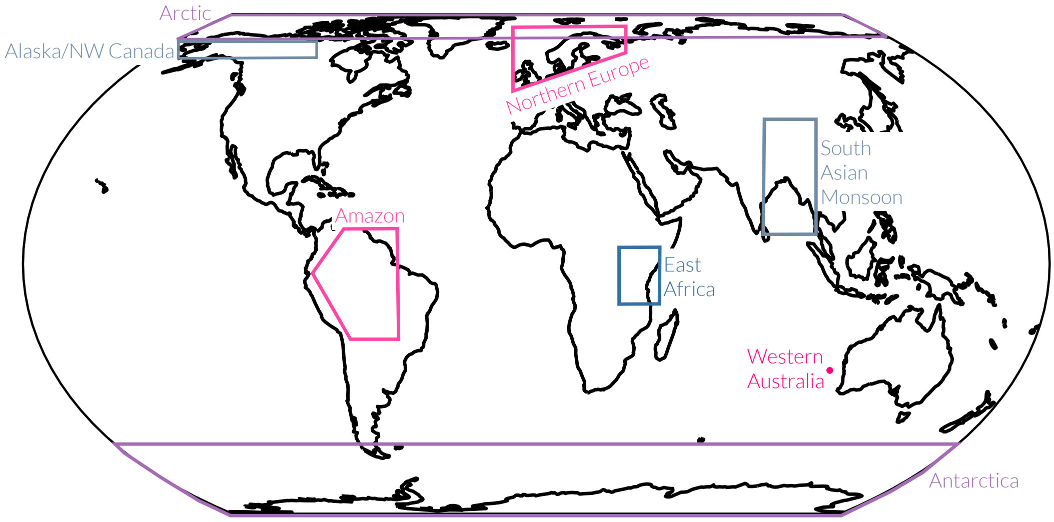

Figure S1. Regions used for panels in Figure 2. Definitions are from IPCC (2013), except for East Africa (Ayugi et al. 2021), South Asian Monsoon (Geen et al. 2020), and Western Australia (Hobday et al. 2016).

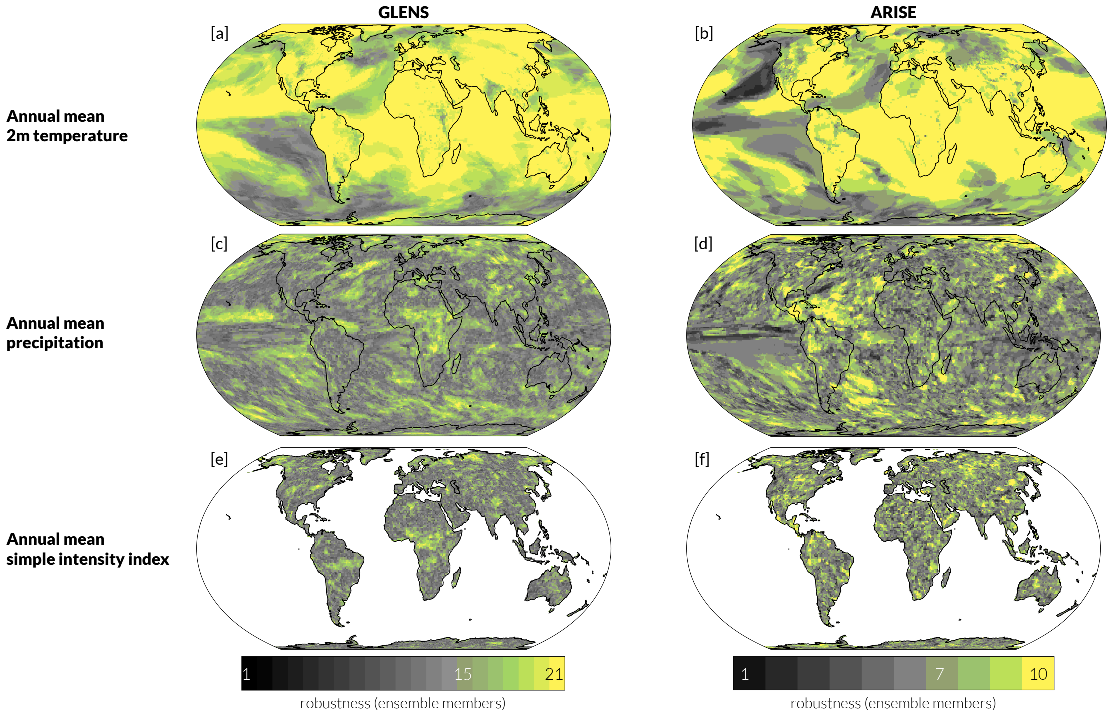

Figure S2. Robustness of data shown in Figures 3-8.

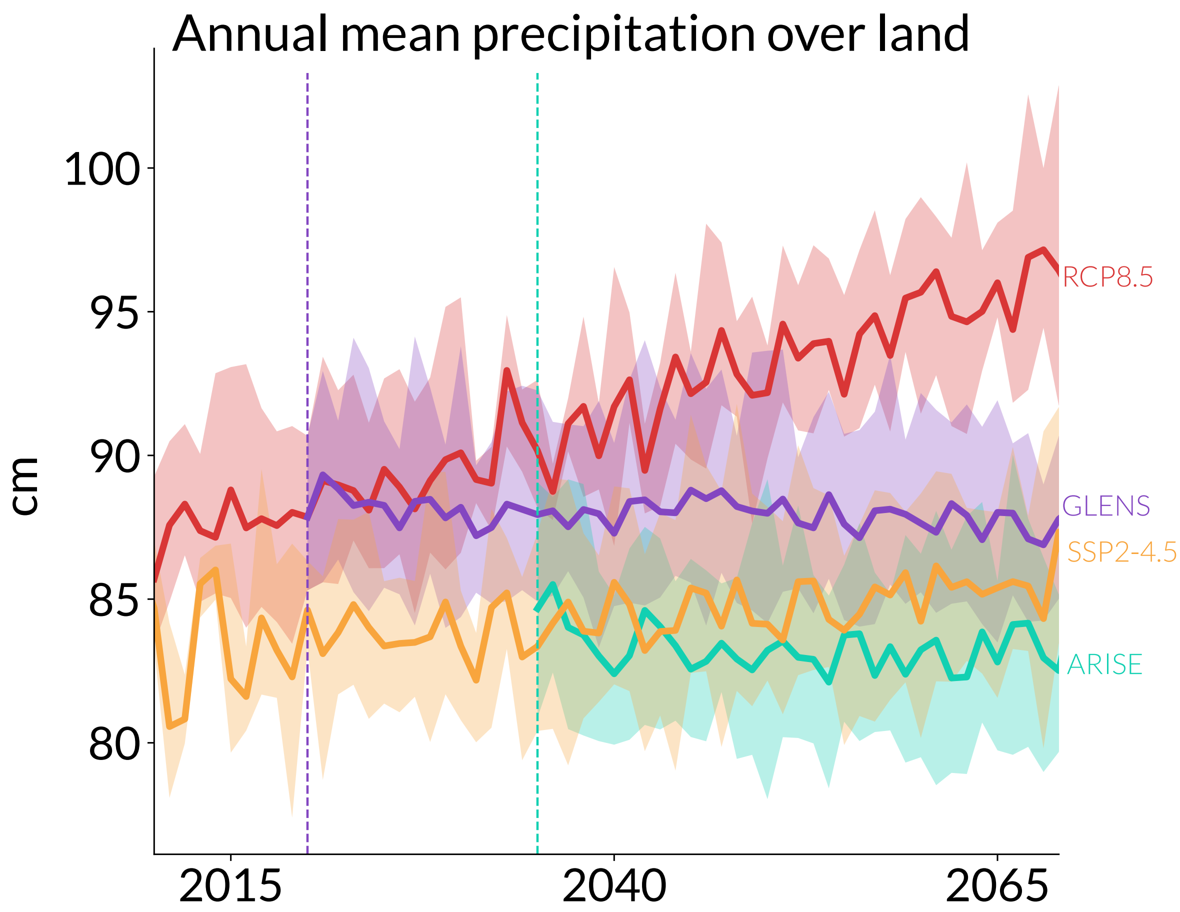

Figure S3. Timeseries of annual mean precipitation over land only in GLENS and ARISE.

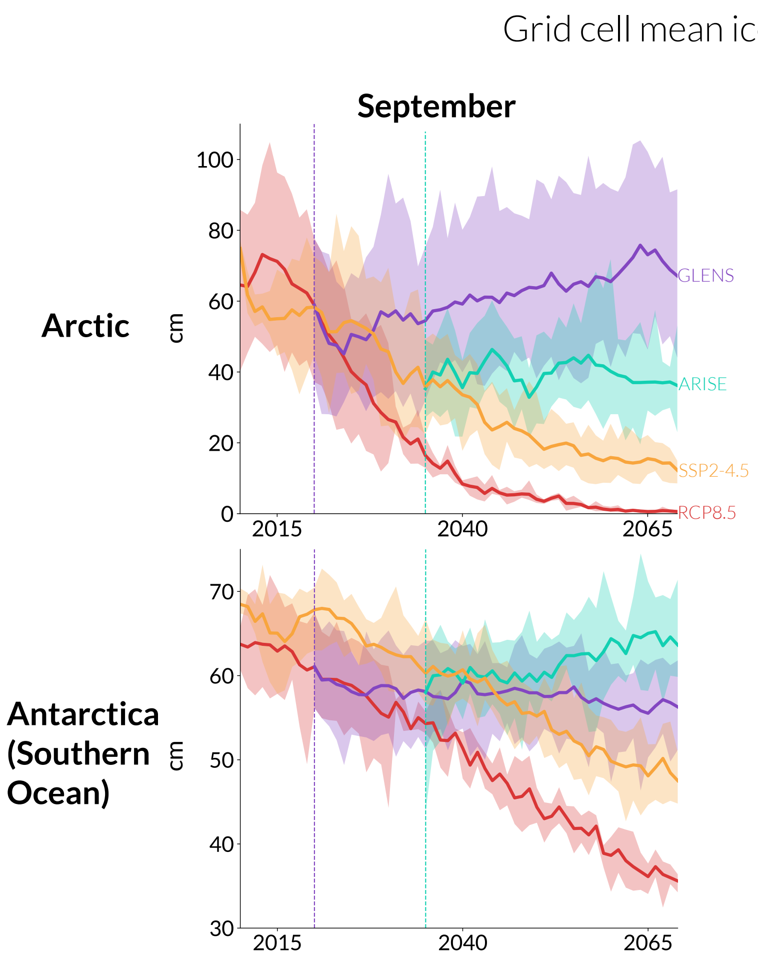

Figure S4. Timeseries of grid cell mean sea ice thickness in GLENS and ARISE.

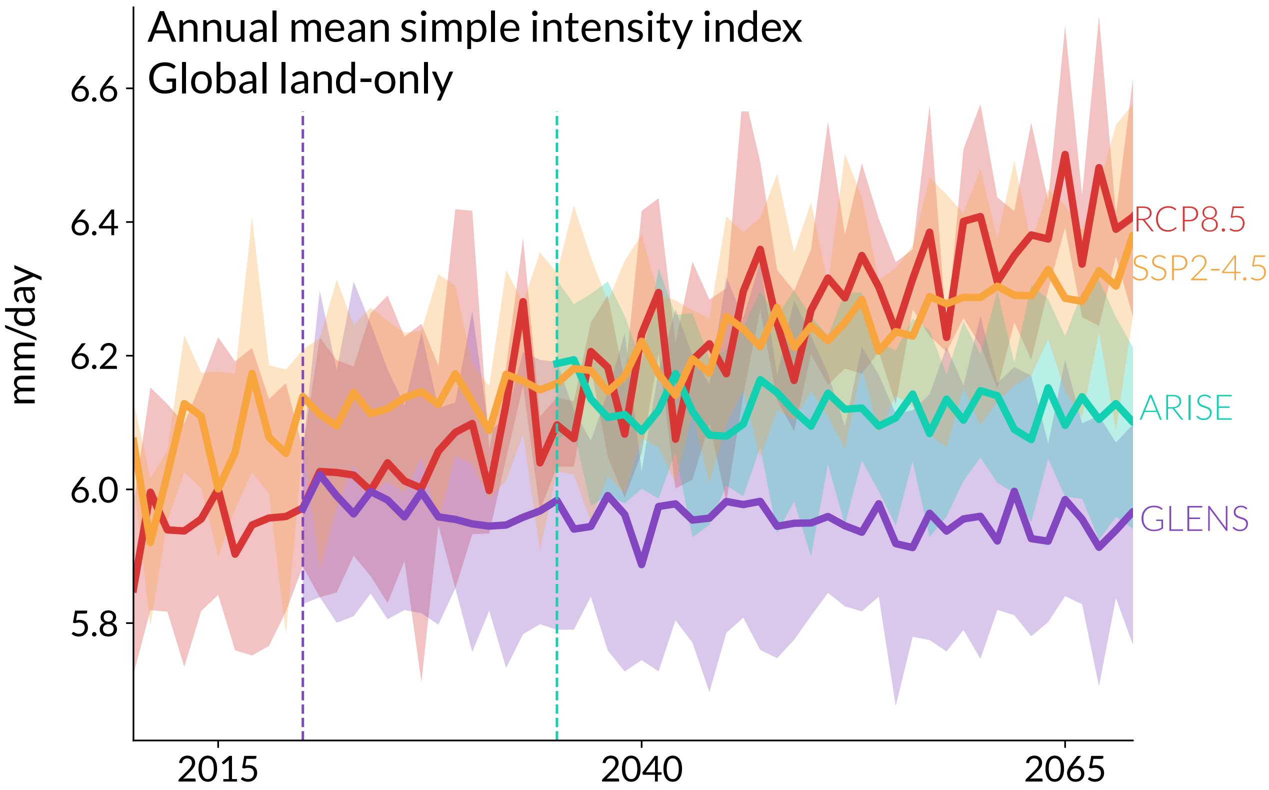

Figure S5. Timeseries of the simple intensity index over land only in GLENS and ARISE.

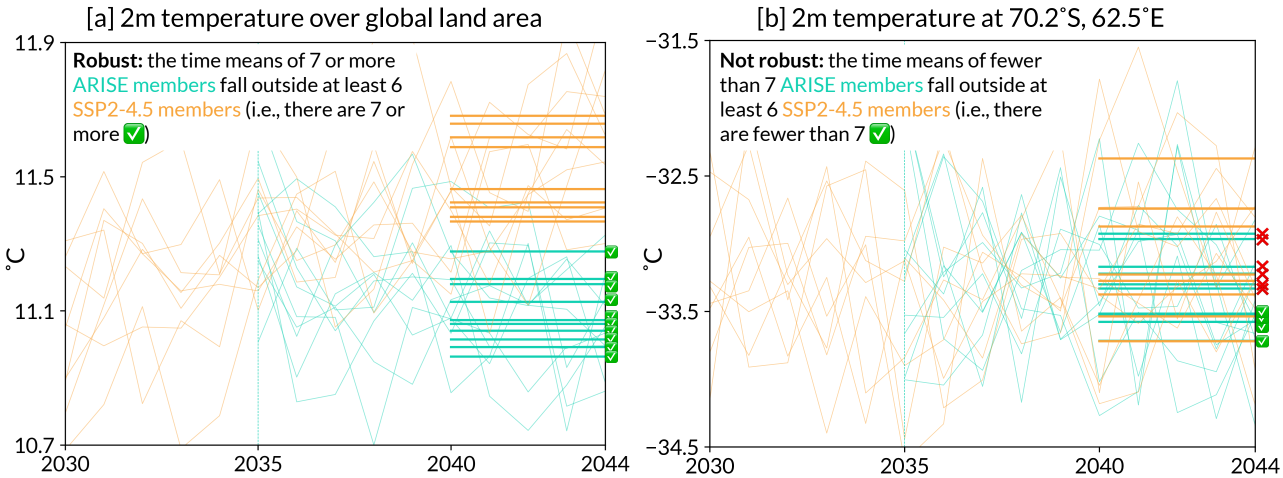

Figure S6. Examples of robust (panel a) and not robust (panel b) timeseries shown for ARISE 2m temperature data. Horizontal bars show the value of the 5-year time means used to compare robustness. Thin solid lines show the timeseries for each ensemble member. Green checkmarks mark each ARISE ensemble member which equals or exceeds the user-defined threshold B number of no-SAI members; red X symbols mark those which do not. The vertical dashed line denotes the year when SAI is deployed in the model.

Assessing Outcomes in Stratospheric Aerosol Injection Scenarios Shortly After Deployment

Daniel M. Hueholt[1], Elizabeth A. Barnes [1], James W. Hurrell[1], Jadwiga H. Richter [2], Lantao Sun[1]

[1]Department of Atmospheric Science, Colorado State University, Fort Collins, CO, USA
[2]Climate and Global Dynamics Laboratory, National Center for Atmospheric Research, Boulder, CO, USA

Key Points:

- We demonstrate two ways to frame results from modeling experiments with parallel SAI and no-SAI large ensembles
- SAI deployment could minimize changes in many high-impact climate variables across spatial scales on policy-relevant time horizons
- Results are scenario- and model-dependent so consistency among different SAI simulations does not imply truth for any general SAI deployment

Corresponding author: Daniel M. Hueholt, `daniel.hueholt@colostate.edu`

Abstract

Stratospheric aerosol injection (SAI) is a proposed form of climate intervention that would release reflective particles into the stratosphere, thereby reducing solar insolation and cooling the planet. The climate response to SAI is not well understood, particularly on short-term time horizons frequently used by decision makers and planning practitioners to assess climate information. We demonstrate two framings to explore the climate response in the decade after SAI deployment in modeling experiments with parallel SAI and no-SAI simulations. The first framing, which we call a snapshot around deployment, displays change over time within the SAI scenarios and applies to the question "What happens before and after SAI is deployed in the model?" The second framing, the intervention impact, displays the difference between the SAI and no-SAI simulations, corresponding to the question "What is the impact of a given intervention relative to climate change with no intervention?" We apply these framings to annual mean 2-meter temperature, precipitation, and a precipitation extreme during the 10 years after deployment in two large ensembles of Earth system model simulations that comprehensively represent both the SAI injection process and climate response, and connect these results to implications for other climate variables. We show that SAI deployment robustly reduces changes in many high-impact climate variables even on these short timescales where the forced response is relatively small, but that details of the climate response depend on the model version, greenhouse gas emissions scenario, and other aspects of the experimental design.

1 Introduction

Despite global pledges and ongoing actions to reduce greenhouse gas emissions, warming from anthropogenic climate change is expected to far exceed the targets set under the Paris Agreement (Matthews & Wynes, 2022). On mid-century time horizons, substantial increases in global temperature are expected to occur both in no-mitigation pathways (Figure 1a) and in more plausible scenarios with moderate mitigation (Figure 1b) (Hausfather & Peters, 2020). Near-term climate risk includes severe impacts to vulnerable communities already disproportionately affected by climate change (e.g., Shearer, 2012; Carr, 2016), as well as terrestrial and marine ecosystems (e.g., Frieler et al., 2013; Panetta et al., 2018; Abatzoglou et al., 2021). Poorly-understood feedbacks involving parts of the Earth system such as clouds, ice, and ecology may worsen climate change or its impacts beyond what is anticipated in current models (e.g. Swann et al., 2010; Genet et al., 2013; Bjordal et al., 2020; King et al., 2020; Gatti et al., 2021; Boulton et al., 2022).

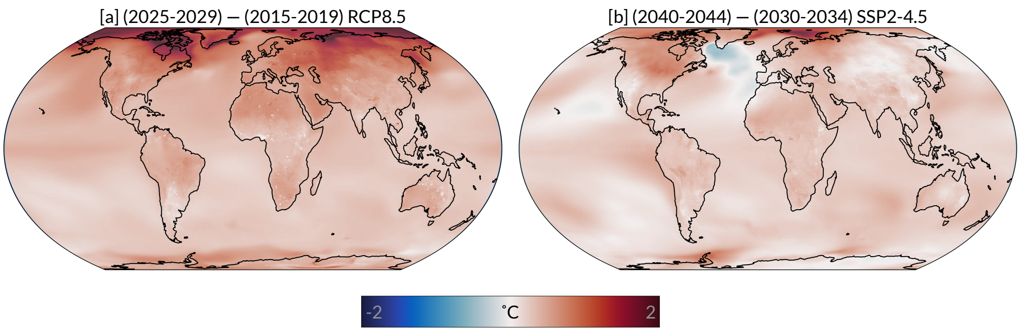

Figure 1. Ensemble mean annual mean 2m temperature change between the snapshot periods in the no-SAI scenarios: RCP8.5 [a] and SSP2-4.5 [b]. See Section 2.1 for description of modeling experiments.

These realities of unavoidable anthropogenic climate change have motivated the study of climate intervention, broadly defined as possible methods to reduce climate risk and impacts through deliberate intervention in the Earth system (The Royal Society, 2009). Stratospheric aerosol injection (SAI) is one proposed climate intervention to release reflective aerosol particles into the upper atmosphere, where the particles would reflect some of the incoming solar radiation and decrease global mean temperature. SAI is inspired by processes that occur naturally after volcanic eruptions and large wildfires (e.g. Timmreck, 2012; Das et al., 2021). SAI does not reduce greenhouse gas emissions, which are the root cause of anthropogenic climate change, but may complement climate change mitigation by reducing climate risk while emissions reductions and carbon removal technologies are implemented (Long & Shepherd, 2014; Buck, 2022). The United States National Academies of Sciences, Engineering, and Medicine (NASEM) have called for the establishment of a transdisciplinary research program on SAI and other proposed solar climate intervention techniques to support informed discussion of these methods (NASEM, 2021).

Global and regional climate responses to SAI are not well understood on the short time horizons of 10 years or fewer often used by decision makers and planning practitioners to assess climate information (e.g., Bolson et al., 2013; DePolt, 2021; Pearman & Cravens, 2022). Previous SAI modeling experiments have provided useful insights into general implications of the intervention, such as the potential for SAI to reduce global mean temperature, the inability of SAI to counteract impacts linked directly to CO_2 concentration, and the risk of rapid climate change if SAI is stopped ("termination shock") (e.g., Rasch et al., 2008; Tilmes et al., 2009; Jones et al., 2013; Bony et al., 2013; Kwiatkowski et al., 2015; Trisos et al., 2018). Many of these experiments (e.g., the Geoengineering Model Intercomparison Project; Kravitz et al. (2011)) have relied on models with limited representations of relevant Earth system processes including atmospheric chemistry, stratospheric dynamics, and aerosol microphysics (e.g., McCusker et al., 2015; Quaglia et al., 2023). Many of the SAI scenarios in these experiments are implemented in highly idealized ways, such as by prescribing the aerosol optical depth fields or reducing the model solar constant (Kravitz et al., 2011), which can produce a very distinct climate response from when SAI is more realistically represented with interactive aerosols (Ferraro et al., 2015; Visioni et al., 2021; Bednarz et al., 2022). These limitations leave large gaps in scientific knowledge of the climate response to SAI scenarios on spatiotemporal scales relevant to policymakers, planning practitioners, and questions of how SAI would affect climate risk inequality (Buck et al., 2014; NASEM, 2021; Pearman & Cravens, 2022).

The Geoengineering Large Ensemble (GLENS, Tilmes, Richter, Kravitz, et al. (2018)) and Assessing Responses and Impacts of Solar climate intervention on the Earth system with stratospheric aerosols (ARISE-SAI-1.5, J. H. Richter et al. (2022)) projects are the first large ensembles of Earth system model simulations that comprehensively represent processes most important to realistically portray SAI and employ strategically-placed SAI to meet specific intervention goals. GLENS and ARISE-SAI-1.5 each contain parallel ensemble simulations: one following a climate change trajectory with no SAI, and one where SAI is deployed. This design helps separate the forced response to SAI from the influence of climate change and internal variability.

The parallel simulations in GLENS and ARISE-SAI-1.5 provide extensive insight into the climate response to SAI. We propose two framings that utilize these parallel simulations to efficiently display multiple perspectives on the climate response to SAI. The first, which we call a snapshot around deployment, displays the change over time within the SAI simulations. This corresponds to the question, "What happens before and after SAI is deployed in the model?" The second, the intervention impact, describes the difference between the SAI and no-SAI simulations. This addresses the question, "What is the impact of a given intervention relative to climate change with no intervention?"

We apply these two framings to explore the climate response to SAI in the decade after SAI is deployed in GLENS and ARISE-SAI-1.5. Using our two framings together allows us to explore both the tangible climate response through the snapshot around deployment and place these changes in context to climate change with no SAI with the intervention impact. We apply our framings to annual mean 2m temperature, annual mean precipitation, and the simple intensity index (a measure of extreme precipitation), and connect these results to global and regional impacts on an assortment of other climate variables selected for their familiarity in Earth science and importance for human and ecological impacts. We discuss commonalities and differences between the climate responses in the GLENS and ARISE-SAI-1.5 scenarios of SAI deployment.

Our work addresses the goals of NASEM (2021) to "advance knowledge relevant to decision making" and "develop policy-relevant knowledge." Consistent with this NASEM report and the broader social science literature, we explicitly distinguish our goals from research on the practical deployment of SAI about which critical ethical and governance concerns exist (Burns et al., 2016; NASEM, 2021). We intend our study simply to support the informed discussion of the potential risks and benefits of SAI.

2 Data and Methods

2.1 Description of Simulations

We use model output from the GLENS (Tilmes, Richter, Kravitz, et al., 2018) and ARISE-SAI-1.5 (hereafter ARISE, (J. H. Richter et al., 2022)) experiments to explore the climate response to SAI. These are large ensembles of SAI modeling experiments performed in fully-interactive Earth system models, with strategically-placed SAI to meet specific temperature targets. We summarize key aspects of the design of GLENS and ARISE, and refer readers to Tilmes, Richter, Kravitz, et al. (2018) and J. H. Richter et al. (2022) for more comprehensive descriptions of the experiments. GLENS and ARISE both employ the Community Earth System Model (CESM) with the Whole Atmosphere Community Climate Model (WACCM) as its atmospheric component, albeit different versions of the model that will be described shortly. WACCM includes 70 vertical layers (model top 140km) to explicitly simulate the stratosphere and lower mesosphere, and uses a 1.25° longitude x 0.9° latitude horizontal resolution. The representation of processes thought to be most important for SAI and its climate response, including stratospheric dynamics, heterogeneous chemistry, and aerosol production, show good agreement with observations of the mean state and anomalous conditions under volcanic aerosol loading (M. J. Mills et al., 2017; J. H. Richter et al., 2017; Gettelman et al., 2019).

Each of the two experiments contains two parallel ensemble simulations: one following a future greenhouse gas forcing scenario with no SAI, and one where SAI is also deployed. A proportional-integral feedback-control algorithm (known as the "controller") annually adjusts the amount of sulfur dioxide continuously released at four latitudes (30° and 15° N/S, all at 180°E) intended to maintain global mean temperature, the pole-to-pole temperature gradient, and the pole-to-equator temperature gradient at some specified target value (MacMartin et al., 2014; Kravitz et al., 2017; MacMartin et al., 2017; MacMartin & Kravitz, 2019). These targets aim to ensure planetary circulations under SAI change less than if only global mean temperature were to be targeted (Tilmes, Richter, Kravitz, et al., 2018; Visioni et al., 2021; Cheng et al., 2022).

GLENS and ARISE each portray a unique intervention scenario where SAI is deployed to maintain specific goals against a particular greenhouse gas forcing. GLENS uses a no-mitigation emissions trajectory (Representative Concentration Pathway [RCP] 8.5; van Vuuren et al. (2011)) with SAI deployed to maintain a global mean temperature target near 2020 values (Tilmes, Richter, Kravitz, et al., 2018). This yields a large signal-to-noise ratio useful to isolate the forced response to the SAI intervention over time.

Table 1. Contrasts key aspects of the experimental design of GLENS and ARISE. Compiled from Tilmes, Richter, Kravitz, et al. (2018) and J. H. Richter et al. (2022).

	GLENS	ARISE
Model version	CESM1(WACCM5)	CESM2(WACCM6)
Ensemble size (SAI)	21 members 2020-2099	10 members 2035-2069
Ensemble size (no-SAI)	21 members 2010-2030, 3 members 2010-2097	5 members 2015-2069, 5 members 2015-2100
Forcing scenario	RCP8.5: No mitigation	SSP2-4.5: Moderate mitigation
Global mean surface temperature target	2015-2024 average of first 13 RCP8.5 members (≈1.1°C above IPCC (2021) preindustrial)	2020-2039 average of first 5 SSP2-4.5 members (≈1.5°C above IPCC (2021) preindustrial)
Temperature gradient targets	2010-2030 mean	2020-2039 mean
SAI deployment year	2020	2035
Injection height	≈25 km	≈21 km

ARISE is run with a moderate-mitigation scenario (Shared Socioeconomic Pathway [SSP] 2-4.5; Riahi et al. (2017)) and a temperature target of approximately 1.5°C above the IPCC AR6 pre-industrial definition (J. H. Richter et al., 2022; IPCC, 2021). ARISE illustrates one plausible future where the use of SAI complements current mitigation strategies to achieve Paris Agreement goals (J. H. Richter et al., 2022).

There are several differences between the experimental design of GLENS and ARISE. We summarize these in Table 1, and provide details on their implications here.

1. **The two experiments use different model versions:** GLENS uses CESM1(WACCM5) while ARISE uses CESM2(WACCM6). Thus, GLENS and ARISE exhibit different spatial patterns of the forced response due to model dependencies, particularly the depiction of subtropical and Southern Ocean low clouds (Gettelman et al., 2019; Fasullo & Richter, 2023). CESM1(WACCM5) is described by Hurrell et al. (2013) and M. J. Mills et al. (2017), and CESM2(WACCM6) by Danabasoglu et al. (2020) and Gettelman et al. (2019).
2. **The two experiments have different forcing scenarios:** GLENS uses RCP8.5 while ARISE uses SSP2-4.5, which yields distinct spatial patterns of the forced response. RCP8.5 and SSP2-4.5 differ in many ways that affect these spatial patterns, including the depiction of land use and aerosol emissions, but the primary influence is the different CO_2 concentration which operates through a direct effect on clouds and precipitation (e.g., Sherwood et al., 2015; Rugenstein et al., 2016; Fasullo & Richter, 2023). These scenario dependencies are largest in the mid-latitudes and subtropics (Fasullo & Richter, 2023).
3. **The GLENS temperature target is the 2015-2024 mean in the RCP8.5 simulations (Tilmes, Richter, Kravitz, et al., 2018), while the ARISE target is the 2020-2039 mean in the SSP2-4.5 simulations (J. H. Richter et al., 2022); SAI is deployed in 2020 in GLENS and 2035 in ARISE.** The effect of differences in temperature target and deployment year are not yet well understood. Targeted modeling experiments to provide insight into these parameters have recently been completed (MacMartin et al., 2022). Due to differences in model physics and definitions of the preindustrial baseline, it is more precise to discuss temperature targets in terms of the time averages implemented in

each experiment. For additional context, we note these global mean temperature targets correspond to approximately 1.1°C above preindustrial in GLENS and 1.5°C in ARISE when the IPCC AR6 definition is used (IPCC, 2021).

4. **The method of generating ensemble spread is different between GLENS and ARISE.** The ocean state in every member of GLENS is branched off the first member of the CESM Large Ensemble (Kay et al., 2015) in which the Atlantic Meridional Overturning Circulation (AMOC) is strengthening. Hence, each realization of GLENS begins with a strengthening state of the AMOC and ensemble spread is generated only through differing atmospheric initial conditions. On the decadal time horizons we emphasize in this study, the memory of these ocean initial conditions has not fully dispersed (Tilmes, Richter, Kravitz, et al., 2018; Fasullo et al., 2018). This increases oceanic heat transport into the North Atlantic and influences European climate (Fasullo et al., 2018). Longer-term trends in AMOC strength may be caused by changes in precipitation that impact salinity and temperature gradients in the ocean (Fasullo & Richter, 2023). In contrast, the ocean states from five separate SSP2-4.5 simulations dispersed over multiple decades are used in addition to differing atmospheric initial conditions to generate ensemble spread in ARISE (J. H. Richter et al., 2022). Thus, ARISE samples ocean internal variability more widely than GLENS.
5. **Aerosol is injected at lower altitudes in GLENS (≈25 km) than in ARISE (≈21 km).** Injection height affects stratospheric chemistry, but has few other effects on the climate as long as the altitude is above the tropopause (Tilmes, Richter, Mills, et al., 2018; Y. Zhang et al., 2022). Injection heights near 20 km are consistent with near-future aerospace technology (D'Oliveira et al., 2016; Moriyama et al., 2017; W. Smith et al., 2022).

Because the controller maintains meridional temperature gradient targets under different spatial patterns of the forced response between GLENS and ARISE, it injects aerosol in disparate latitudinal amounts throughout each experiment. This leads to distinct global distributions of aerosol optical depth (Figure 1 in Fasullo and Richter (2023)) with corresponding differences in the regional climate response. These model and scenario dependencies imply that the results of GLENS and ARISE are specific to these scenarios; consistency of a result between the simulations does not imply increased confidence that the result is true of any general SAI deployment. Thus, GLENS and ARISE are best compared to illuminate the differences in the climate response produced by two SAI scenarios simulated in physically comprehensive models.

2.2 Analysis Metrics

We use the five years prior to SAI deployment (2015-2019 in GLENS, 2030-2034 in ARISE) as pre-intervention reference periods, and the five-year period beginning five years after deployment (2025-2029 in GLENS, 2040-2044 in ARISE) as a post-intervention reference period while remaining close to the deployment year. The ensemble sizes of the GLENS and ARISE experiments (Table 1) increase the number of years available for analysis, allowing us to average over many realizations of relatively short spans of time (Deser et al., 2012; Maher et al., 2021; Tebaldi et al., 2021). We develop two framings to investigate the climate response to SAI. Our first framing, which we call a snapshot around deployment, depicts change over time within the SAI experiments: the difference between 2025-2029 and 2015-2019 in GLENS, and 2040-2044 and 2030-2034 in ARISE. This can be phrased as answering the question: "What happens before and after SAI is deployed in the model?" Our second framing, the intervention impact, is the SAI and no-SAI difference for the 2025-2029 period in GLENS and the 2040-2044 period in ARISE. This can be expressed as answering the question: "What is the impact of a given intervention relative to climate change with no intervention?" This was inspired by the "world avoided" perspective used to study the Montreal Protocol (e.g., Morgenstern et al., 2008).

We structure our framings to focus on the short-term climate responses occurring in the first 10 years after SAI deployment. This near-term timeframe has been analyzed with respect to the atmospheric dynamical response to SAI (e.g., Tilmes et al., 2017; H. Richter Jadwiga et al., 2018), but has seen little exploration with respect to climate impacts. Policymakers and planning practitioners often assess climate information on time horizons of 10 years or fewer (e.g., Bolson et al., 2013; DePolt, 2021; Pearman & Cravens, 2022; Keys et al., 2022). Thus, we portray our results consistently with how information could hypothetically be used for decisions about SAI deployment, governance, and evaluation. The signal-to-noise ratio of the forced response to SAI is smaller on this time horizon than when trends are calculated over a longer span of time. We use timeseries (Figure 2) to complement ensemble mean global maps of our two framings (Figures 3-8). These allow us to display the longer-term evolution of a variable and emphasize the contribution of internal variability for a specific region. The longer-term evolution may be different from the short-term response, and helps place our work in context to previous results in the literature. We show timeseries for 2010-2069 to span the period where output from both GLENS and ARISE are available. We use the CESM2(WACCM6) Historical simulations (Danabasoglu et al., 2020) to supplement the period 2010-2014 before the ARISE no-SAI simulations begin.

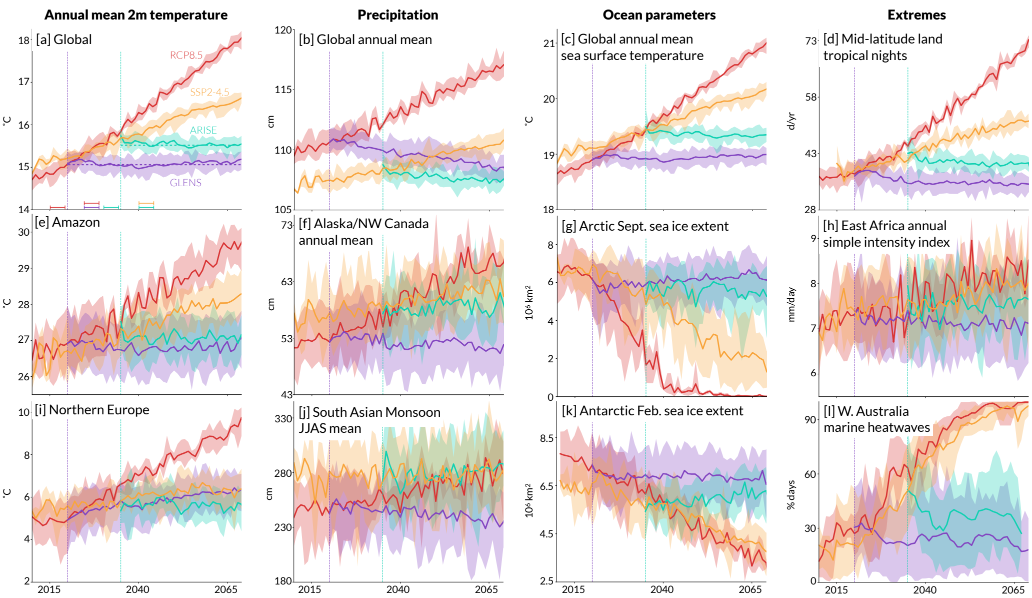

Figure 2. Timeseries of selected climate variables in the GLENS and ARISE experiments. Bold line shows the ensemble mean for each scenario; shading illustrates the range of the ensemble members given by the maximum and minimum values at each year. The vertical dotted lines mark the deployment of SAI in 2020 (GLENS) and 2035 (ARISE). Horizontal dashed lines in Figure 2a denote the global mean temperature target in GLENS and ARISE. Brackets in Figure 2a highlight the time periods used to define the snapshot around deployment and intervention impact. See Methods for detailed descriptions of variables and regions.

As an Earth system model, CESM provides a breadth of model output including variables that represent the atmosphere, ocean, land surface, and ecology. This allows for many aspects of the Earth system response to SAI to be assessed holistically. We examined a wide variety of variables in developing this paper. Here, we present a subset that are familiar in climate science, have links to human impacts, and whose representation in CESM has been evaluated against observations (Hurrell et al., 2013; Danabasoglu et al., 2020; Fasullo, 2020). We describe our selected variables below.

Surface temperature: We calculate annual mean 2-meter temperature from monthly output. For temperature and all other variables, we define regions following the IPCC Working Group 1 Fifth Assessment Report Annex (van Oldenborgh et al., 2013), except when specified otherwise. We illustrate the regions we discuss in this work in Figure S1. In addition to the regions highlighted in Figure 2, we provide timeseries of 2-meter annual mean temperature for all IPCC-defined regions in the archive linked in Supporting Information Text S2.

Tropical nights: We use tropical nights from the World Climate Research Program's Expert Team on Climate Change Detection and Indices (ETCCDI) set of extreme indices as an example of a temperature extreme. Tropical nights is the annual count of days where minimum temperature exceeds 20°C (68°F) (X. Zhang et al., 2011). High nighttime temperatures increase mortality, particularly in urban areas without widespread air conditioning (Buechley et al., 1972; Sillmann & Roeckner, 2008; Laaidi et al., 2012; Rathi et al., 2021). We calculate tropical nights from daily minimum temperature using Pyclimdex (Groenke, 2022). Tye et al. (2022) comprehensively explore ETCCDI extremes in GLENS; no such assessment has been completed for ARISE.

Sea surface temperature (SST): We calculate annual mean SST from monthly output at the surface level of the ocean component in CESM.

Marine heatwaves: We identify marine heatwaves as events where daily mean SST exceeds the daily local 90th percentile (computed over 2010-2020) for longer than 5 days (Hobday et al., 2016; Oliver, 2022). This definition is standard in public communication and the scientific literature (e.g., Benthuysen et al., 2018; Holbrook et al., 2020; MHIWG, 2022). Marine heatwaves occur at many locations around the world (K. E. Smith et al., 2021), and we select a point in the Leeuwin Current (30.63°S, 112.5°E) where they have been frequently observed to harm local ecology (Chandrapavan et al., 2019; Holbrook et al., 2020). We apply a left-aligned 5-year rolling sum of days to smooth interannual variability in Figure 2l.

Sea ice extent: We show sea ice extent in its minimum month for both hemispheres – September for the Arctic and February for the Antarctic (Stroeve et al., 2012; Parkinson, 2019). Sea ice extent is the sum of grid cell areas with ice fraction greater than 0.15 in the atmospheric component of CESM (NSIDC, 2020).

Precipitation: We derive annual mean precipitation from monthly total precipitation. To describe South Asian Monsoon rainfall, we use the conventional dynamical definition of June through September mean precipitation between 10°N to 40°N and 80°E to 100°E (Geen et al., 2020). We provide timeseries of annual mean precipitation for all IPCC-defined regions at the archive provided in the Supporting Information Text S2.

Simple intensity index: We use the ETCCDI simple intensity index to illustrate changes in a precipitation extreme. The simple intensity index measures the precipitation amount divided by the number of days with precipitation (X. Zhang et al., 2011). This is a standard metric to analyze trends in precipitation intensity (e.g., Alexander et al., 2006; Ayugi et al., 2021). Following Ayugi et al. (2021), we define the East African region as spanning 12°S to 5°N and 28°E to 42°E to capture relevant regional climate features. We calculate the simple intensity index using Pyclimdex (Groenke, 2022).

2.3 Robustness

Regional trends in the model output are due to combinations of the forced response to the SAI intervention, the direct effect of CO_2 concentration, and internal variability (Fasullo & Richter, 2023). We define a metric called *robustness (ρ)* to quantify where the signal from the forced response to SAI is large relative to noise from internal variability and the response to climate change. Because the parallel ensemble simulations in GLENS and ARISE are identical aside from the presence of the SAI intervention, consistent differences between the SAI and no-SAI members are likely due to the response to the SAI intervention. Robustness quantifies this consistency as the count ρ of each SAI realization whose temporal mean over a given time period falls outside (exceeds or subceeds) a user-defined quantity of no-SAI realizations (denoted as B; $B = 11$ for GLENS, $B = 6$ for ARISE given differing ensemble sizes [Table 1]).

Sufficiently large values of robustness indicate a consistent ("robust") forced response to the SAI intervention. We refer to results as "robust" if they fall outside the 90% confidence bounds of the robustness distribution expected by chance (i.e. robustness distribution computed via 10,000 pairs of vectors randomly sampled from a uniform distribution). "Robust" results have $\rho \geq 15$ members in GLENS and $\rho \geq 7$ members in ARISE. These thresholds are statistically significant at the $p < 0.1$ level ($p = 0.02$ for GLENS, $p = 0.05$ for ARISE) under a binomial test–however, we emphasize that the exact choice of threshold is subjective. We apply image muting to de-emphasize (gray out) points that are not robust ($\rho < 15$ members for GLENS, $\rho < 7$ members for ARISE) without removing data from our maps (Tomkins et al., 2022).

To help build intuition, we provide an example of results considered robust and not robust for a case where the SAI ensemble members subceed the no-SAI members (Figure S6). Robustness is a non-parametric test that leverages the parallel large ensemble design of GLENS and ARISE to rigorously convey the consistency of a result, without requiring assumptions about the statistical distribution of the variable of interest.

We formalize robustness mathematically in Equation 1. For each longitude θ and latitude ϕ (grid point), we compute the robustness $\rho_{\theta,\phi}$ which is the maximum of the number of SAI realizations that exceed or subceed B number of no-SAI realizations. $\overline{S_{\theta,\phi_{r_z}}}$ is the time mean over a given period for a variable for each SAI realization r_z, $\overline{\tilde{S}_{\theta,\phi_{r_{\{B\}}}}}$ denotes time means of a variable for B number of no-SAI realizations $r_{\{B\}}$, and Z is the size of the SAI ensemble. The robustness calculation is repeated for every latitude and longitude to generate a map of robustness for a given variable (Figure S2).

$$\rho_{\theta,\phi} = \max\left(\left\{\mathrm{n}\left(r_{S_{\theta,\phi_{r_z}} > \overline{\tilde{S}_{\theta,\phi_{r_{\{B\}}}}}}\right), \mathrm{n}\left(r_{S_{\theta,\phi_{r_z}} < \overline{\tilde{S}_{\theta,\phi_{r_{\{B\}}}}}}\right)\right\}, \middle| \forall z \in \{0, ..., Z\}\right) \qquad (1)$$

The unit of robustness is "number of ensemble members" inherited from the cardinality operator n(). Robustness is non-negative and bounded by the size of the SAI ensemble: $\rho_{\theta,\phi} = Z$ is the upper bound (21 in GLENS, 10 in ARISE). We detail the algorithm to calculate robustness and the binomial test for statistical significance in Supplementary Information Text S1.

3 Results

GLENS and ARISE both maintain global mean temperature close to their respective target values, while the no-SAI RCP8.5 and no-SAI SSP2-4.5 scenarios continue warming globally throughout the period (Figure 2a). Thus, global mean temperature shows a clear forced response to the SAI intervention. For each timeseries shown in Figure 2, the envelope around the ensemble mean illustrates a range of internal climate variability by spanning the maximum to minimum value across the ensemble at each year. The ensemble sizes for each scenario differ and are given in Table 1. While forced trends are visible in the ensemble mean for many of the timeseries (Figure 2), internal climate variability is substantial especially for regional scales and noisier variables such as precipitation (e.g., Figure 2h). The ensemble spreads of the SAI and no-SAI scenarios overlap for all quantities in the time periods shortly after deployment when the forced response is small. Thus, internal variability can mask the forced response to the SAI intervention for any individual realization. Our results suggest climate variability may lead to the "perceived failure" of SAI on short time horizons across many variables (Figure

2) regardless of the true forced response from SAI, as previously shown for temperature alone (Keys et al., 2022).

We use global maps corresponding to the snapshot around deployment and intervention impact framings (Figures 3-8, see Methods for details) to explore the ensemble mean response of temperature, precipitation, and the simple intensity index within the decade after SAI deployment. We refer to timeseries in Figure 2 to connect results from our framings to the evolution of a variable over a longer period of time and to display the spread due to internal variability.

3.1 What Happens Before and After SAI is Deployed in the Model?

We begin our discussion with 2-meter temperature (Figure 3), as it is the variable directly targeted by the SAI intervention. Some global warming is visible in the GLENS snapshot (Figure 3a) due to the rapid warming rate in the underlying RCP8.5 emissions trajectory. The GLENS experimental design maintains global mean temperature at 2020 levels, which leaves some warming relative to the 2015-2019 mean which defines our pre-intervention snapshot baseline. The SSP2-4.5 forcing scenario used in ARISE yields a much more moderate rate of warming as compared to RCP8.5 and a smaller relative change between the 2030-2034 baseline and the deployment of SAI in 2035. Hence, the snapshot around deployment for ARISE does not display substantial planetary-scale warming.

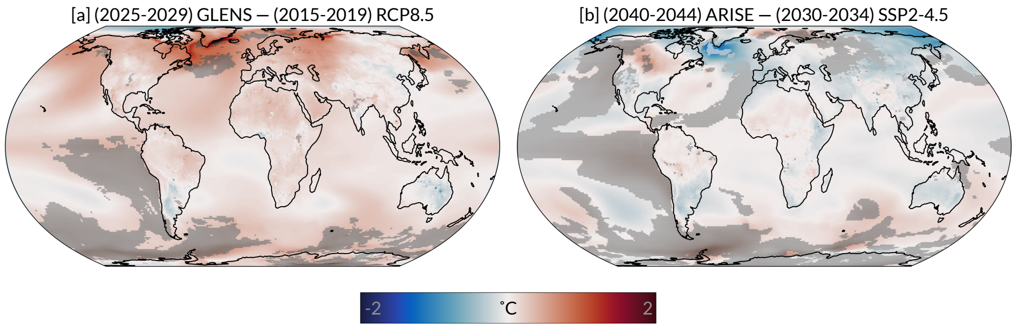

Figure 3. Ensemble mean annual mean 2m temperature change for the snapshot around deployment within the SAI scenarios: GLENS [a] and ARISE [b]. Regions shown in color are robust (fall outside the 90% confidence bounds of the robustness distribution expected by chance), while regions with gray shading are not robust (fall within the 90% confidence bounds of the robustness distribution expected by chance). See Section 2.3 for details.

The subpolar North Atlantic Ocean stands out as the region experiencing the largest temperature trends (Figure 3). The sign of the trend is opposite in each experiment: warming in GLENS (Figure 3a), but cooling in ARISE (Figure 3b). This difference is driven by the opposite-signed AMOC evolution in GLENS and ARISE. The strengthening AMOC throughout the simulation period in GLENS increases oceanic heat transport into the North Atlantic (Fasullo et al., 2018); in contrast, the AMOC weakens in ARISE, although it remains stronger than in the no-SAI SSP2-4.5 scenario (J. H. Richter et al., 2022; Fasullo & Richter, 2023). These trends in the AMOC are likely due to memory of the ocean initial conditions on the short timescales shown in the snapshot around deployment (Tilmes, Richter, Kravitz, et al., 2018; Fasullo et al., 2018). On a longer time horizon, the direct effect of CO_2 concentration on precipitation may drive a forced response in the AMOC by altering oceanic salinity and temperature gradients (Fasullo & Richter, 2023); however, this long-term effect would not be visible in our snapshot around deployment.

In general, regional changes in annual mean 2m temperature after SAI deployment are much smaller in GLENS and ARISE (Figure 3) than in no-SAI RCP8.5 and no-SAI SSP2-4.5 (Figure 1). All regions (save Northern Europe in GLENS, discussed shortly) defined by the IPCC WG1-AR5 Atlas (van Oldenborgh et al., 2013) have a similar temperature response over time to the global mean. We provide 2m annual mean temperature timeseries for each IPCC region at the archive linked in Supporting Information Text S2 to illustrate the universality of this response. We highlight the Amazon region (Figure 2e) as an example of the typical evolution of annual mean temperatures on a regional scale. The response in the Amazon is very similar to the global response: GLENS and ARISE are maintained near their pre-deployment values, while the no-SAI scenarios continue to warm through the period. Temperature trends are robust for all land area in GLENS outside Antarctica, and almost all land area in ARISE. We reiterate that "robust" trends fall outside the 90% confidence bounds of the distribution expected by chance, and a full description of the robustness metric can be found in Section 2.3.

Northern Europe (Figure 2i) experiences moderate warming throughout the period in GLENS. While this warming has been previously shown to occur on late-century timescales (Tilmes, Richter, Kravitz, et al., 2018; Fasullo et al., 2018; Banerjee et al., 2021), we show this warming is already robust within the decade after deployment (Figure 3a). One cause of this warming may be a forced positive trend in the North Atlantic Oscillation driven by stratospheric heating from the absorption of radiation by the sulfate aerosols injected by the SAI intervention (Banerjee et al., 2021). The strengthening AMOC could also contribute to this regional warming by importing heat from lower latitudes (Fasullo et al., 2018). In contrast, we find Northern European warming does not occur in ARISE on any timescale (Figure 2i, 3b). The differing responses in Northern Europe emphasize that climate responses in an individual scenario may be particular to that strategy, and cannot be assumed to be general features of all SAI interventions.

We now turn to the snapshot around deployment for precipitation (Figure 4). Due to its large internal variability (Deser et al., 2012), fewer regional trends are robust for precipitation rather than temperature on our short timescale of 10 years after SAI deployment. Precipitation robustly decreases over portions of the tropical Pacific in GLENS (Figure 4a). On longer timescales, similar trends emerge over much of the basin and are responsible for a decrease in globally-averaged precipitation (Figure 2b). Since these changes primarily affect precipitation over the ocean, land-only precipitation trends in GLENS are small even later into the century (Figure S3). The decrease in tropical oceanic precipitation may be related to the direct effect of CO_2 concentration in the RCP8.5 emissions pathway or the circulation response to stratospheric heating, but the precise underlying dynamics are not well understood (Bony et al., 2013; Simpson et al., 2019). Trends in global precipitation in ARISE are difficult to identify (Figure 2b), which indicates a more moderate injection strategy may minimize impacts on the global hydrologic cycle.

The location of equatorial precipitation associated with the Intertropical Convergence Zone (ITCZ) shifts southward in GLENS and ARISE (Figure 4), but we show these changes are not robust on the short timescale of 10 years after deployment. The controller in GLENS and ARISE minimizes the impacts on the ITCZ by maintaining the pole-to-pole and pole-to-equator temperature gradients which are primarily responsible for ITCZ location (Kang et al., 2018; Undorf et al., 2018; Cheng et al., 2022). Other processes such as differences in the relative aerosol burden between the Northern and Southern Hemispheres, changes in heat transport by the AMOC, or stratospheric heating can still influence ITCZ location (Haywood et al., 2013; Iles & Hegerl, 2014; Moreno-Chamarro et al., 2019; Ciemer et al., 2021; Cheng et al., 2022). Thus, on longer timescales, the controller reduces but cannot fully eliminate shifts in the ITCZ location (Cheng et al., 2022).

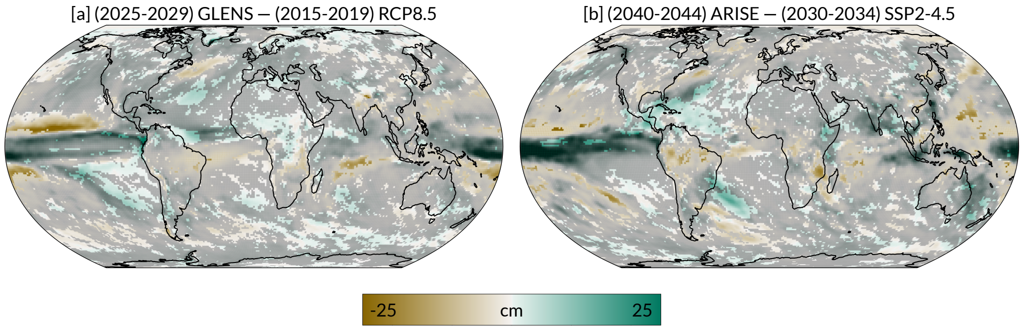

Figure 4. Ensemble mean annual mean precipitation change for the snapshot around deployment within the SAI scenarios: GLENS [a] and ARISE [b]. Regions shown in color are robust (fall outside the 90% confidence bounds of the robustness distribution expected by chance), while regions with gray shading are not robust (fall within the 90% confidence bounds of the robustness distribution expected by chance). See Section 2.3 for details.

Targeted modeling experiments and observations after volcanic eruptions indicate that much larger ITCZ migrations are possible under SAI strategies that do not consider planetary temperature gradients (Haywood et al., 2013; Cheng et al., 2022). ITCZ location can be targeted more successfully in simulations that use different controller targets specifically tuned to this feature (Lee et al., 2020).

Early modeling results indicated certain SAI strategies could cause large decreases in South Asian Monsoon precipitation (Robock et al., 2008). Any changes to the monsoon directly affect water availability and agricultural productivity in a densely populated region, with further impacts on global food supply (Gadgil & Rupa Kumar, 2006; Kulkarni et al., 2016). We find that South Asian Monsoon precipitation robustly decreases in GLENS (Figure 4a) even on the short timescales of the snapshot around deployment, although the magnitude of the change is smaller than the increase throughout the period in no-SAI RCP8.5 (Figure 2j). Late in the century in GLENS, monsoon failures double in frequency due to circulation changes induced by stratospheric heating from the extremely large aerosol burden (Simpson et al., 2019). In contrast, South Asian Monsoon precipitation remains largely unchanged in both SSP2-4.5 and ARISE across short (Figure 4b) and long timescales (Figure 2j). Thus, we conclude that impacts on monsoon precipitation are dependent on the SAI strategy rather than a general feature of this type of intervention. Visioni et al. (2020) previously showed monsoon impacts varied in modeling experiments where SAI was limited to certain seasons. The difference in base state between the CESM2 SSP2-4.5 and CESM1 RCP8.5 simulations indicate that model dependencies and the greenhouse forcing scenario may be especially important to the monsoonal climate response.

On our short time horizon of the decade after deployment, global changes in the simple intensity index are very noisy without clear forced responses (Figure 5). This illustrates how internal climate variability can remain the dominant driver of certain high-impact climate variables after SAI deployment. Precipitation extremes exhibit the largest internal variability of any quantity examined here. The 10-member ensemble of ARISE, in particular, is not sufficient to isolate the forced response to SAI on precipitation extremes for regional spatial scales and short timescales after deployment. An ensemble size of 40 members or more may be necessary to reliably isolate forced trends (Kirchmeier-Young & Zhang, 2020).

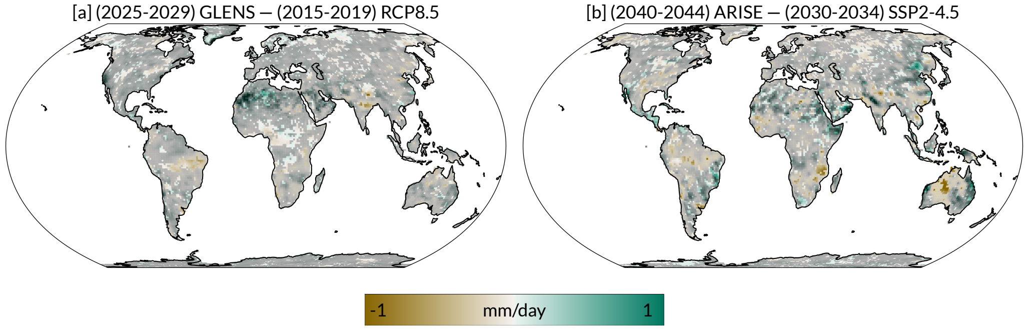

Figure 5. Ensemble mean annual mean simple intensity index change for the snapshot around deployment within the SAI scenarios: GLENS [a] and ARISE [b]. Regions shown in color are robust (fall outside the 90% confidence bounds of the robustness distribution expected by chance), while regions with gray shading are not robust (fall within the 90% confidence bounds of the robustness distribution expected by chance). See Section 2.3 for details.

3.2 What is the Impact of a Given Intervention Relative to Climate Change with no Intervention?

GLENS and ARISE both avert warming around the globe (Figure 6); that is, they robustly remain cooler than their respective no-SAI scenarios. This impact is evident even in the decade immediately following deployment and is nearly single-signed worldwide (Figure 6). The Arctic experiences the greatest averted warming (Figure 6), because the controller greatly reduces Arctic amplification by maintaining the pole-to-equator temperature gradient in addition to global mean temperature. In either GLENS or ARISE, no regions experience robust warming relative to climate change in the ensemble mean. Regions that warm relative to a pre-intervention baseline, namely Northern Europe in GLENS, still experience averted warming relative to climate change (Figure 6a). This illustrates the value of using our two framings together: the snapshot around deployment shows the tangible climate response, while the intervention impact places these changes in context to climate change with no SAI.

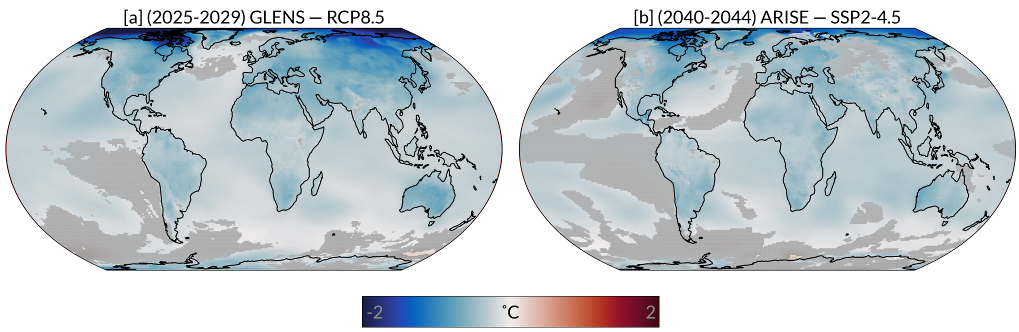

Figure 6. Ensemble mean intervention impact (SAI - no-SAI difference) for annual mean 2m temperature: GLENS [a] and ARISE [b]. Regions shown in color are robust (fall outside the 90% confidence bounds of the robustness distribution expected by chance), while regions with gray shading are not robust (fall within the 90% confidence bounds of the robustness distribution expected by chance). See Section 2.3 for details.

In highly localized areas where trends are weak in both the SAI and no-SAI scenarios, the intervention impact is small and noise from internal variability can make it appear as if the intervention has exacerbated warming. This effect can be seen in very small portions of the Southern Ocean in GLENS (Figure 6a) and the northeastern Pacific Ocean in ARISE (Figure 6b) that display a positively-signed intervention impact. Note these regional features are not robust and thus are grayed out. Internal variability may mask the impact of SAI for any individual realization, which complicates how the effectiveness of an intervention could be perceived on short timescales after deployment (Keys et al., 2022).

We connect the averted warming in global mean temperature to implications for the evolution over time of other Earth system variables. Global sea surface temperature (Figure 2c) responds very similarly to global 2m temperature (Figure 2a). Sea ice loss is halted in the Arctic and Antarctic (Figure 2g, Figure 2k) in both GLENS and ARISE. The impact is most dramatic in GLENS; in no-SAI RCP8.5, the Arctic experiences ice-free minima by mid-century while SAI keeps sea ice near present-day values. The SAI scenarios have the potential to slow or avert feedbacks involving sea and land ice. Arctic sea ice thickness is maintained alongside sea ice extent (Figure S4), indicating ice-insulation feedbacks that can cause rapid sea ice loss (e.g., Burt et al., 2016) could be averted. In Antarctica, preventing sea ice loss prevents the exposure of coastal ice shelves to ocean waves which may make land ice less likely to collapse (Massom et al., 2018). Exploring impacts from SAI on the cryosphere in more depth is a clear avenue for future research.

Mid-latitude tropical nights increase drastically in the no-SAI scenarios (Figure 2d) and are associated with the planetary-scale expansion of the tropics (Rajaud & Noblet-Ducoudré, 2017). SAI interventions in GLENS and ARISE both limit this process, maintaining tropical nights near pre-intervention values. Averting increases in tropical nights could mitigate impacts from heat waves, as high overnight temperatures worsen mortality during these events (e.g., Buechley et al., 1972; Laaidi et al., 2012). While heat extremes are mitigated under GLENS or ARISE, extreme cold may be worsened relative to no-SAI climate change scenarios (Tye et al., 2022). More detailed risk analysis is necessary to quantify tradeoffs in exposure to extreme cold and heat.

Temperature extremes in the ocean are also impacted by the averted warming under SAI. In GLENS and ARISE, increases in marine heatwave frequency are prevented for a point off the coast of Western Australia (Figure 2l). In the no-SAI scenarios, this location reaches a near-permanent marine heatwave state by mid-century. Marine ecosystems are increasingly affected by compound hazards: combinations of stressors including direct anthropogenic impacts, ocean acidification, and temperature extremes (e.g., Chandrapavan et al., 2019; Gruber et al., 2021). While SAI only mitigates temperature extremes, lessening one component of compound hazards may allow ecosystems to stay within their capacity for resilience (Bernhardt & Leslie, 2013).

Due to the large internal variability of precipitation (Deser et al., 2012), regional impacts are not robust over much of the globe in the decade after deployment (Figure 7). Robust regional precipitation responses are particularly difficult to identify in ARISE (Figure 7b), as both the ensemble size and SAI forcing are smaller than in GLENS. Still, certain impacts of the SAI intervention on precipitation oppose notable no-SAI climate change trends. For example, precipitation in the Southern Hemisphere subtropics decreases in response to climate change when meridional SST gradients in the South Pacific Ocean are impacted by the rate of change in global mean temperature (Sniderman et al., 2019). As GLENS and ARISE both maintain global mean temperatures, they avert this transient climate response (Figure 7).

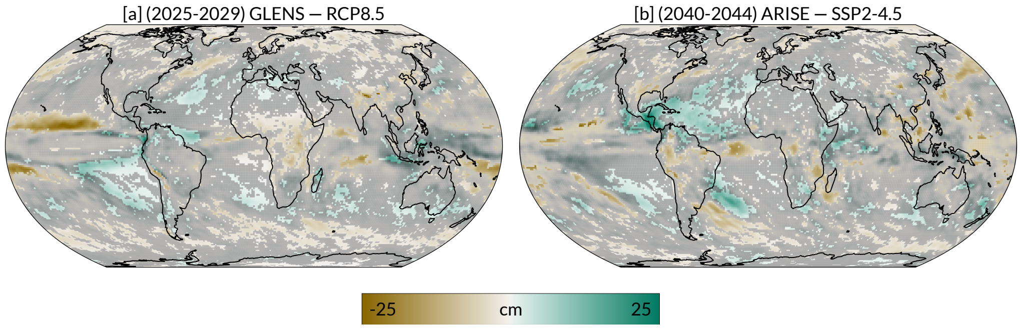

Figure 7. Ensemble mean intervention impact (SAI - no-SAI difference) for annual mean precipitation: GLENS [a] and ARISE [b]. Regions shown in color are robust (fall outside the 90% confidence bounds of the robustness distribution expected by chance), while regions with gray shading are not robust (fall within the 90% confidence bounds of the robustness distribution expected by chance). See Section 2.3 for details.

GLENS and ARISE both robustly oppose increases in precipitation in portions of the Arctic that occur in the no-SAI scenarios (Figure 7) associated with rapid warming from Arctic amplification (Figure 2f). Warmer air temperatures support exponentially larger saturation vapor pressures, a trend which is reinforced by increased evaporation from the open ocean due to sea ice loss (Bogerd et al., 2020). Alaska Native communities are highly vulnerable to climate change impacts, particularly those from increased precipitation (Shearer, 2012; Melvin et al., 2017). The potential to avert these impacts indicates SAI could mitigate regional climate risk inequality in certain cases, although far more analysis is needed to draw any broader conclusions. Increased temperature and precipitation together yield more vegetation growth in the Arctic (Elmendorf et al., 2012; Dial et al., 2022). Arctic vegetation can exacerbate warming by decreasing surface albedo and increasing local water vapor mixing ratios, which accelerates ice loss and encourages further plant growth (Swann et al., 2010). This positive feedback is considered a possible tipping point in the Earth system (Crump et al., 2021; Heijmans et al., 2022). SAI may prevent this process by preventing increases in temperature and precipitation, although further research would be necessary to examine this in detail.

As discussed previously, changes in the simple intensity index are largely not robust (Figure 8) due to the influence of internal variability. Still, certain robust regional impacts are more apparent relative to climate change in the intervention impact than relative to the pre-intervention baseline in the snapshot around deployment. Globally, GLENS and ARISE both reduce the simple intensity index over land relative to the no-SAI scenarios (Figure 8, Figure S5). We highlight the East African region, specifically, due to its high exposure to extreme precipitation events (Adhikari et al., 2015; Nicholson, 2017; Wainwright et al., 2021). The simple intensity index decreases in East Africa relative to no-SAI climate change, although this trend is robust for only a portion of the area on the timescale of 10 years after SAI deployment. Over the course of the simulation period, regional simple intensity index decreases in GLENS and is maintained in ARISE (Figure 2h) in contrast to increasing trends in the no-SAI scenarios. Elsewhere, regional trends in the simple intensity index are generally not robust. We provide time-series of the simple intensity index for each IPCC-defined region in the archive linked in Supporting Information Text S2.

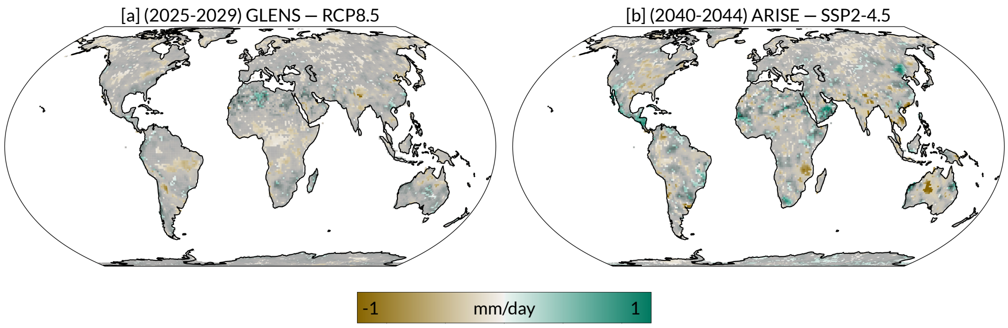

Figure 8. Ensemble mean intervention impact (SAI - no-SAI difference) for annual mean simple intensity index: GLENS [a] and ARISE [b]. Regions shown in color are robust (fall outside the 90% confidence bounds of the robustness distribution expected by chance), while regions with gray shading are not robust (fall within the 90% confidence bounds of the robustness distribution expected by chance). See Section 2.3 for details.

4 Conclusions

We present two ways to frame output from Earth system modeling experiments with parallel intervention and no-intervention ensemble simulations, which we call the snapshot around deployment and the intervention impact. Our framings directly address the research questions: "What happens before and after the intervention is deployed in the model?" and "What is the impact of a given intervention relative to climate change with no intervention?" We apply our framings to GLENS and ARISE, the first SAI modeling experiments performed by large ensembles of fully-interactive Earth system models. We explore these questions in the decade after SAI deployment, a policy-relevant time horizon that has not been widely explored in the literature with respect to SAI impacts. We use our framings to efficiently describe many aspects of the climate response to SAI, including 2-meter temperature, annual mean precipitation, and the simple intensity index (a measure of precipitation extremes). We observe certain commonalities between the SAI scenarios relative to their respective no-SAI scenarios: annual mean temperature is maintained at target values after deployment both globally and for nearly all IPCC-defined regions, sea ice loss is halted at both poles, and increases in certain marine and terrestrial heat extremes are prevented. However, GLENS and ARISE each portray a distinct scenario of SAI deployment with its own design and climate response. Results that are consistent between the simulations still cannot be taken to be true of any general SAI deployment.

Our study is the first to synthesize results from GLENS and ARISE together. We focus on a short-term time horizon of the 10 years after deployment, which is consistent with timescales frequently used by policymakers and planning practitioners to assess climate information (e.g., Bolson et al., 2013; DePolt, 2021; Pearman & Cravens, 2022; Keys et al., 2022). This differentiates our work from existing literature on the climate response in GLENS or ARISE, which usually examines time horizons later in the century in order to obtain a larger forced signal from the SAI intervention (e.g., Tilmes, Richter, Kravitz, et al., 2018; Simpson et al., 2019; Pinto et al., 2020; Camilloni et al., 2022; J. H. Richter et al., 2022; Tye et al., 2022). We intend our data analysis to provide a point of entry for researchers or educators unfamiliar with SAI, and include an archive of timeseries depicting each of the variables used with our framings for all IPCC regions (linked in Supporting Information Text S2).

Our framings can be used with any modeling experiment that has parallel intervention and no-intervention simulations. In particular, we see an opportunity to apply these framings to planned ARISE-SAI experiments that explore a wider variety of temperature targets, deployment dates, and Earth system models (MacMartin et al., 2022). As our framings directly address concrete questions of the climate response to SAI, they could also motivate a more comprehensive regional risk analysis constructed in collaboration with planning practitioners and members of affected communities (e.g., Adelekan & Asiyanbi, 2016; DePolt, 2021).

We show that while large forced responses to SAI are visible in the ensemble mean within the decade after deployment in GLENS and ARISE, internal variability can mask impacts in individual realizations. The noise from internal variability has important implications for three key open problems highlighted by NASEM (2021): detection, monitoring, and social perception of any climate intervention. Machine learning methods have shown promise for rapid detection of the surface climate response to SAI despite the influence of internal variability (Barnes et al., 2022). Improved understanding of the data most useful to detect SAI could help constrain potential observational platforms for long-term monitoring. Regardless of the true forced climate response, the noise from internal variability may influence the perceived success or failure of any climate intervention – or climate action more broadly (Keys et al., 2022; Diffenbaugh et al., 2022).

GLENS and ARISE provide high-fidelity depictions of two useful scientific knowledge-building scenarios (Talberg et al., 2018). However, these scenarios are geopolitically idealized: they depict SAI as an uninterrupted worldwide project ("global action" scenarios) with a controller limiting disruptions to global mean climate. Thus, the results from these specific scenarios do not generalize to any given SAI intervention. The differences between GLENS and ARISE demonstrate that even global action scenarios with many commonalities can produce distinct climate responses, due to factors such as model dependency, the ocean initial conditions, and the direct effects of the underlying greenhouse gas emissions forcing scenario. To explore a scenario of interest, it will be necessary to explicitly model that scenario; the results cannot be assumed to track those of GLENS or ARISE. Future modeling should widely explore the scenario design space, with possible examples of candidates including unilateral ("rogue actor") deployment and environmental peacebuilding (Fitzgerald, 2016; Buck, 2022).

5 Open Research

The processed model output used throughout this work, code for reproducibility, and additional timeseries described in Supporting Information Text S2 are archived at the Open Science Foundation (Hueholt, 2022, doi.org/10.17605/OSF.IO/5A2ZF). This repository additionally includes a datasheet describing the data adapted from best practices from software engineering (Gebru et al., 2021).

The original GLENS model dataset from which the data in this work was derived can be obtained from NCAR (Tilmes & Richter, 2018, doi.org/10.5065/D6JH3JXX).

The original ARISE dataset from which the data in this work was derived (all SAI members and 5 no-SAI members) are located on the NCAR Climate Data Gateway (J. H. Richter, 2022, doi.org/10.5065/9kcn-9y79). The remaining 5 no-SAI members are available from the NCAR Climate Data Gateway at (M. Mills et al., 2022, doi.org/10.26024/0cs0-ev98). All ARISE data may also be accessed from Amazon Web Services (NCAR, 2022, registry.opendata.aws/ncar-cesm2-arise/).

The complete CESM2(WACCM6) Historical runs from which the data in this work was derived are available at Earth System Grid (Danabasoglu, 2019, doi.org/10.22033/ESGF/CMIP6.11298).

Acknowledgments

The GLENS and ARISE datasets were produced and maintained by the National Center for Atmospheric Research (NCAR). We extend special thanks to Charlotte Connolly and Ariel Morrison for constructive comments and feedback on data visualization, to Mari Tye for early insight on useful metrics of climate extremes, and to Hui Li for clarification about AMOC definitions. We additionally thank Ben Kravitz and one anonymous reviewer for providing thoughtful and timely comments that improved the work.

This work was supported by the LAD Climate Fund, and the Defense Advanced Research Projects Agency (DARPA, grant no. HR00112290071). The views, opinions, and/or findings expressed are those of the authors and should not be interpreted as representing the official views or policies of the Department of Defense or the U.S. government. DMH was additionally supported by the National Science Foundation (NSF) Graduate Research Fellowship (grant no. 006784). This material is based upon work supported by NCAR, which is a major facility sponsored by NSF under Cooperative Agreement no. 1852977. The GLENS experiment was supported by DARPA funding, and ARISE by SilverLining through the Safe Climate Research Initiative. CESM2(WACCM6) Historical was produced by NCAR. The CESM project is supported primarily by NSF.

References

Abatzoglou, J. T., Battisti, D. S., Williams, A. P., Hansen, W. D., Harvey, B. J., & Kolden, C. A. (2021, November). Projected increases in western US forest fire despite growing fuel constraints. *Commun Earth Environ*, *2*(1), 1–8. Retrieved 2022-08-12, from `http://www.nature.com/articles/s43247-021-00299-0` (Number: 1 Publisher: Nature Publishing Group) doi: 10.1038/s43247-021-00299-0

Adelekan, I. O., & Asiyanbi, A. P. (2016, January). Flood risk perception in flood-affected communities in Lagos, Nigeria. *Nat Hazards*, *80*(1), 445–469. Retrieved 2022-08-05, from `https://doi.org/10.1007/s11069-015-1977-2` doi: 10.1007/s11069-015-1977-2

Adhikari, U., Pouyan Nejadhashemi, A., & R. Herman, M. (2015). A Review of Climate Change Impacts on Water Resources in East Africa. *Transactions of the ASABE*, *58*(6), 1493–1507. Retrieved from `https://elibrary.asabe.org/abstract.asp?aid=46551&t=3` (Place: St. Joseph, MI Publisher: ASABE) doi: 10.13031/trans.58.10907

Alexander, L. V., Zhang, X., Peterson, T. C., Caesar, J., Gleason, B., Klein Tank, A. M. G., … Vazquez-Aguirre, J. L. (2006). Global observed changes in daily climate extremes of temperature and precipitation. *Journal of Geophysical Research: Atmospheres*, *111*(D5). Retrieved 2022-05-18, from `http://onlinelibrary.wiley.com/doi/abs/10.1029/2005JD006290` (_eprint: https://agupubs.onlinelibrary.wiley.com/doi/pdf/10.1029/2005JD006290) doi: 10.1029/2005JD006290

Ayugi, B., Dike, V., Ngoma, H., Babaousmail, H., Mumo, R., & Ongoma, V. (2021, January). Future Changes in Precipitation Extremes over East Africa Based on CMIP6 Models. *Water*, *13*(17), 2358. Retrieved 2022-02-16, from `https://www.mdpi.com/2073-4441/13/17/2358` (Number: 17 Publisher: Multidisciplinary Digital Publishing Institute) doi: 10.3390/w13172358

Banerjee, A., Butler, A. H., Polvani, L. M., Robock, A., Simpson, I. R., & Sun, L. (2021, May). Robust winter warming over Eurasia under stratospheric sulfate geoengineering – the role of stratospheric dynamics. *Atmospheric Chemistry and Physics*, *21*(9), 6985–6997. Retrieved 2021-05-07, from `https://acp.copernicus.org/articles/21/6985/2021/` (Publisher: Copernicus GmbH) doi: 10.5194/acp-21-6985-2021

Barnes, E. A., Hurrell, J. W., & Sun, L. (2022). Detecting changes in global extremes under the GLENS-SAI climate intervention strategy. *Geophysical Research Letters*, *n/a*(n/a), e2022GL100198. Retrieved 2022-10-19, from https://onlinelibrary.wiley.com/doi/abs/10.1029/2022GL100198 (_eprint: https://onlinelibrary.wiley.com/doi/pdf/10.1029/2022GL100198) doi: 10.1029/2022GL100198

Bednarz, E. M., Visioni, D., Banerjee, A., Braesicke, P., Kravitz, B., & MacMartin, D. G. (2022). The Overlooked Role of the Stratosphere Under a Solar Constant Reduction. *Geophysical Research Letters*, *49*(12), e2022GL098773. Retrieved 2022-06-25, from http://onlinelibrary.wiley.com/doi/abs/10.1029/2022GL098773 (_eprint: https://agupubs.onlinelibrary.wiley.com/doi/pdf/10.1029/2022GL098773) doi: 10.1029/2022GL098773

Benthuysen, J. A., Oliver, E. C. J., Feng, M., & Marshall, A. G. (2018). Extreme Marine Warming Across Tropical Australia During Austral Summer 2015–2016. *Journal of Geophysical Research: Oceans*, *123*(2), 1301–1326. Retrieved 2022-05-19, from http://onlinelibrary.wiley.com/doi/abs/10.1002/2017JC013326 (_eprint: https://agupubs.onlinelibrary.wiley.com/doi/pdf/10.1002/2017JC013326) doi: 10.1002/2017JC013326

Bernhardt, J. R., & Leslie, H. M. (2013). Resilience to climate change in coastal marine ecosystems. *Annual review of marine science*, *5*(1), 371–392.

Bjordal, J., Storelvmo, T., Alterskjær, K., & Carlsen, T. (2020, November). Equilibrium climate sensitivity above 5 °C plausible due to state-dependent cloud feedback. *Nat. Geosci.*, *13*(11), 718–721. Retrieved 2021-09-02, from http://www.nature.com/articles/s41561-020-00649-1 (Bandiera_abtest: a Cg_type: Nature Research Journals Number: 11 Primary_atype: Research Publisher: Nature Publishing Group Subject_term: Atmospheric chemistry;Climate and Earth system modelling;Projection and prediction Subject_term_id: atmospheric-chemistry;climate-and-earth-system-modelling;projection-and-prediction) doi: 10.1038/s41561-020-00649-1

Bogerd, L., van der Linden, E. C., Krikken, F., & Bintanja, R. (2020). Climate State Dependence of Arctic Precipitation Variability. *Journal of Geophysical Research: Atmospheres*, *125*(8), e2019JD031772. Retrieved 2022-07-18, from http://onlinelibrary.wiley.com/doi/abs/10.1029/2019JD031772 (_eprint: https://agupubs.onlinelibrary.wiley.com/doi/pdf/10.1029/2019JD031772) doi: 10.1029/2019JD031772

Bolson, J., Martinez, C., Breuer, N., Srivastava, P., & Knox, P. (2013, August). Climate information use among southeast US water managers: beyond barriers and toward opportunities. *Reg Environ Change*, *13*(1), 141–151. Retrieved 2022-08-08, from https://doi.org/10.1007/s10113-013-0463-1 doi: 10.1007/s10113-013-0463-1

Bony, S., Bellon, G., Klocke, D., Sherwood, S., Fermepin, S., & Denvil, S. (2013, June). Robust direct effect of carbon dioxide on tropical circulation and regional precipitation. *Nature Geosci*, *6*(6), 447–451. Retrieved 2022-07-28, from http://www.nature.com/articles/ngeo1799 (Number: 6 Publisher: Nature Publishing Group) doi: 10.1038/ngeo1799

Boulton, C. A., Lenton, T. M., & Boers, N. (2022, March). Pronounced loss of Amazon rainforest resilience since the early 2000s. *Nat. Clim. Chang.*, *12*(3), 271–278. Retrieved 2022-03-21, from http://www.nature.com/articles/s41558-022-01287-8 (Number: 3 Publisher: Nature Publishing Group) doi: 10.1038/s41558-022-01287-8

Buck, H. J. (2022). Environmental Peacebuilding and Solar Geoengineering. *Frontiers in Climate*, *4*. Retrieved 2022-05-03, from https://www.frontiersin.org/article/10.3389/fclim.2022.869774

Buck, H. J., Gammon, A. R., & Preston, C. J. (2014). Gender and Geoengineering. *Hypatia*, *29*(3), 651–669. Retrieved 2021-01-13, from http://onlinelibrary.wiley.com/doi/abs/10.1111/hypa.12083 (_eprint: https://onlinelibrary.wiley.com/doi/pdf/10.1111/hypa.12083) doi: https://doi.org/10.1111/hypa.12083

Buechley, R. W., Van Bruggen, J., & Truppi, L. E. (1972, March). Heat island = death island? *Environmental Research*, *5*(1), 85–92. Retrieved 2022-05-18, from https://www.sciencedirect.com/science/article/pii/0013935172900229 doi: 10.1016/0013-9351(72)90022-9

Burns, E. T., Flegal, J. A., Keith, D. W., Mahajan, A., Tingley, D., & Wagner, G. (2016, November). What do people think when they think about solar geoengineering? A review of empirical social science literature, and prospects for future research. *Earth's Future*, *4*(11), 536–542. Retrieved 2021-06-09, from http://agupubs.onlinelibrary.wiley.com/doi/full/10.1002/2016EF000461 (Publisher: John Wiley & Sons, Ltd) doi: 10.1002/2016EF000461

Burt, M. A., Randall, D. A., & Branson, M. D. (2016, January). Dark Warming. *Journal of Climate*, *29*(2), 705–719. Retrieved 2021-11-12, from http://journals.ametsoc.org/view/journals/clim/29/2/jcli-d-15-0147.1.xml (Publisher: American Meteorological Society Section: Journal of Climate) doi: 10.1175/JCLI-D-15-0147.1

Camilloni, I., Montroull, N., Gulizia, C., & Saurral, R. I. (2022). La Plata Basin Hydroclimate Response to Solar Radiation Modification With Stratospheric Aerosol Injection. *Frontiers in Climate*, *4*. Retrieved 2022-05-03, from https://www.frontiersin.org/article/10.3389/fclim.2022.763983

Carr, W. A. (2016). *Vulnerable populations' perspectives on climate engineering* (Ph.D., University of Montana, United States – Montana). Retrieved 2021-06-14, from http://www.proquest.com/docview/1782319888/abstract/546F9F23A0494EFBPQ/1 (ISBN: 9781339626918)

Chandrapavan, A., Caputi, N., & Kangas, M. I. (2019). The Decline and Recovery of a Crab Population From an Extreme Marine Heatwave and a Changing Climate. *Frontiers in Marine Science*, *6*. Retrieved 2022-05-12, from https://www.frontiersin.org/article/10.3389/fmars.2019.00510

Cheng, W., MacMartin, D. G., Kravitz, B., Visioni, D., Bednarz, E. M., Xu, Y., ... Deng, X. (2022, April). Changes in Hadley circulation and intertropical convergence zone under strategic stratospheric aerosol geoengineering. *npj Clim Atmos Sci*, *5*(1), 1–11. Retrieved 2022-05-11, from http://www.nature.com/articles/s41612-022-00254-6 (Number: 1 Publisher: Nature Publishing Group) doi: 10.1038/s41612-022-00254-6

Ciemer, C., Winkelmann, R., Kurths, J., & Boers, N. (2021, October). Impact of an AMOC weakening on the stability of the southern Amazon rainforest. *Eur. Phys. J. Spec. Top.*, *230*(14), 3065–3073. Retrieved 2022-08-03, from https://doi.org/10.1140/epjs/s11734-021-00186-x doi: 10.1140/epjs/s11734-021-00186-x

Crump, S. E., Fréchette, B., Power, M., Cutler, S., de Wet, G., Raynolds, M. K., ... Miller, G. H. (2021, March). Ancient plant DNA reveals High Arctic greening during the Last Interglacial. *Proceedings of the National Academy of Sciences*, *118*(13), e2019069118. Retrieved 2022-07-18, from https://www.pnas.org/doi/abs/10.1073/pnas.2019069118 (Publisher: Proceedings of the National Academy of Sciences) doi: 10.1073/pnas.2019069118

Danabasoglu, G. (2019). *NCAR CESM2-WACCM-FV2 model output prepared for CMIP6 CMIP historical.* World Climate Research Program. Retrieved 2022-12-16, from https://doi.org/10.22033/ESGF/CMIP6.11298 (Publisher: Earth System Grid Federation Type: dataset)

Danabasoglu, G., Lamarque, J.-F., Bacmeister, J., Bailey, D. A., DuVivier, A. K., Edwards, J., ... Strand, W. G. (2020). The Community Earth System Model Version 2 (CESM2). *Journal of Advances in Modeling Earth Systems*, *12*(2), e2019MS001916. Retrieved 2021-09-08, from http://agupubs.onlinelibrary.wiley.com/doi/abs/10.1029/2019MS001916 (_eprint: https://onlinelibrary.wiley.com/doi/pdf/10.1029/2019MS001916) doi: 10.1029/2019MS001916

Das, S., Colarco, P. R., Oman, L. D., Taha, G., & Torres, O. (2021, August). The long-term transport and radiative impacts of the 2017 British Columbia pyrocumulonimbus smoke aerosols in the stratosphere. *Atmospheric Chemistry and Physics*, *21*(15), 12069–12090. Retrieved 2022-08-16, from https://acp.copernicus.org/articles/21/12069/2021/ (Publisher: Copernicus GmbH) doi: 10.5194/acp-21-12069-2021

DePolt, K. T. (2021). *Analyzing Drivers of Compound Coastal Water Events (CCWE) with Copulas: A Case Study in Eastern North Carolina* (Master's thesis, East Carolina University, Greenville, NC). Retrieved 2022-08-05, from http://hdl.handle.net/10342/9730 (Accepted: 2022-02-10T15:12:25Z Publisher: East Carolina University)

Deser, C., Phillips, A., Bourdette, V., & Teng, H. (2012, February). Uncertainty in climate change projections: the role of internal variability. *Clim Dyn*, *38*(3), 527–546. Retrieved 2022-05-19, from https://doi.org/10.1007/s00382-010-0977-x doi: 10.1007/s00382-010-0977-x

Dial, R. J., Maher, C. T., Hewitt, R. E., & Sullivan, P. F. (2022, August). Sufficient conditions for rapid range expansion of a boreal conifer. *Nature*, 1–6. Retrieved 2022-08-12, from http://www.nature.com/articles/s41586-022-05093-2 (Publisher: Nature Publishing Group) doi: 10.1038/s41586-022-05093-2

Diffenbaugh, N. S., Barnes, E. A., & Keys, P. W. (2022). *Probability of continued local-scale warming and extreme events during and after decarbonization.* ResearchSquare. doi: https://doi.org/10.21203/rs.3.rs-1902791/v1

D'Oliveira, F., Melo, F., & Devezas, T. (2016, August). High-Altitude Platforms - Present Situation and Technology Trends. *Journal of Aerospace Technology and Management*, *8*, 249–262. doi: 10.5028/jatm.v8i3.699

Elmendorf, S. C., Henry, G. H. R., Hollister, R. D., Björk, R. G., Boulanger-Lapointe, N., Cooper, E. J., ... Wipf, S. (2012, June). Plot-scale evidence of tundra vegetation change and links to recent summer warming. *Nature Clim Change*, *2*(6), 453–457. Retrieved 2022-07-18, from http://www.nature.com/articles/nclimate1465 (Number: 6 Publisher: Nature Publishing Group) doi: 10.1038/nclimate1465

Fasullo, J. T. (2020, August). Evaluating simulated climate patterns from the CMIP archives using satellite and reanalysis datasets using the Climate Model Assessment Tool (CMATv1). *Geoscientific Model Development*, *13*(8), 3627–3642. Retrieved 2022-09-15, from https://gmd.copernicus.org/articles/13/3627/2020/ (Publisher: Copernicus GmbH) doi: 10.5194/gmd-13-3627-2020

Fasullo, J. T., & Richter, J. H. (2023, January). Dependence of strategic solar climate intervention on background scenario and model physics. *Atmospheric Chemistry and Physics*, *23*(1), 163–182. Retrieved 2023-01-06, from https://acp.copernicus.org/articles/23/163/2023/ (Publisher: Copernicus GmbH) doi: 10.5194/acp-23-163-2023

Fasullo, J. T., Tilmes, S., Richter, J. H., Kravitz, B., MacMartin, D. G., Mills, M. J., & Simpson, I. R. (2018, December). Persistent polar ocean warming in a strategically geoengineered climate. *Nature Geosci*, *11*(12), 910–914. Retrieved 2022-05-18, from http://www.nature.com/articles/s41561-018-0249-7 (Number: 12 Publisher: Nature Publishing Group) doi: 10.1038/s41561-018-0249-7

Ferraro, A. J., Charlton-Perez, A. J., & Highwood, E. J. (2015). Stratospheric dynamics and midlatitude jets under geoengineering with space mirrors and sulfate and titania aerosols. *Journal of Geophysical Research: Atmospheres*, *120*(2), 414–429. Retrieved 2022-11-03, from https://onlinelibrary.wiley.com/doi/abs/10.1002/2014JD022734 (_eprint: https://onlinelibrary.wiley.com/doi/pdf/10.1002/2014JD022734) doi: 10.1002/2014JD022734

Fitzgerald, M. (2016). Prison or Precaution: Unilateral, State-Mandated Geoengineering under Principles of International Environmental Law. *N.Y.U. Envtl. L.J.*, *24*(2), [i]–282. Retrieved 2022-08-05, from https://heinonline.org/HOL/P?h=hein.journals/nyuev24&i=262

Frieler, K., Meinshausen, M., Golly, A., Mengel, M., Lebek, K., Donner, S. D., & Hoegh-Guldberg, O. (2013, February). Limiting global warming to 2 °C is unlikely to save most coral reefs. *Nature Clim Change*, *3*(2), 165–170. Retrieved 2022-08-12, from http://www.nature.com/articles/nclimate1674 (Number: 2 Publisher: Nature Publishing Group) doi: 10.1038/nclimate1674

Gadgil, S., & Rupa Kumar, K. (2006). The Asian monsoon—agriculture and economy. In *The Asian Monsoon* (pp. 651–683). Springer.

Gatti, L. V., Basso, L. S., Miller, J. B., Gloor, M., Gatti Domingues, L., Cassol, H. L. G., ... Neves, R. A. L. (2021, July). Amazonia as a carbon source linked to deforestation and climate change. *Nature*, *595*(7867), 388–393. Retrieved 2022-06-14, from http://www.nature.com/articles/s41586-021-03629-6 (Number: 7867 Publisher: Nature Publishing Group) doi: 10.1038/s41586-021-03629-6

Gebru, T., Morgenstern, J., Vecchione, B., Vaughan, J. W., Wallach, H., III, H. D., & Crawford, K. (2021, November). Datasheets for datasets. *Commun. ACM*, *64*(12), 86–92. Retrieved 2022-12-12, from https://doi.org/10.1145/3458723 doi: 10.1145/3458723

Geen, R., Bordoni, S., Battisti, D. S., & Hui, K. (2020). Monsoons, ITCZs, and the Concept of the Global Monsoon. *Reviews of Geophysics*, *58*(4), e2020RG000700. Retrieved 2021-08-31, from http://agupubs.onlinelibrary.wiley.com/doi/abs/10.1029/2020RG000700 (_eprint: https://onlinelibrary.wiley.com/doi/pdf/10.1029/2020RG000700) doi: 10.1029/2020RG000700

Genet, H., McGuire, A. D., Barrett, K., Breen, A., Euskirchen, E. S., Johnstone, J. F., ... Yuan, F. (2013, October). Modeling the effects of fire severity and climate warming on active layer thickness and soil carbon storage of black spruce forests across the landscape in interior Alaska. *Environ. Res. Lett.*, *8*(4), 045016. Retrieved 2021-07-13, from https://doi.org/10.1088/1748-9326/8/4/045016 (Publisher: IOP Publishing) doi: 10.1088/1748-9326/8/4/045016

Gettelman, A., Mills, M. J., Kinnison, D. E., Garcia, R. R., Smith, A. K., Marsh, D. R., ... Randel, W. J. (2019). The Whole Atmosphere Community Climate Model Version 6 (WACCM6). *Journal of Geophysical Research: Atmospheres*, *124*(23), 12380–12403. Retrieved 2022-05-17, from http://onlinelibrary.wiley.com/doi/abs/10.1029/2019JD030943 (_eprint: https://agupubs.onlinelibrary.wiley.com/doi/pdf/10.1029/2019JD030943) doi: 10.1029/2019JD030943

Groenke, B. (2022, March). *pyclimdex.* Retrieved 2022-05-18, from https://github.com/bgroenks96/pyclimdex (original-date: 2020-01-23T06:37:54Z)

Gruber, N., Boyd, P. W., Frölicher, T. L., & Vogt, M. (2021, December). Biogeochemical extremes and compound events in the ocean. *Nature*, *600*(7889), 395–407. Retrieved 2022-07-18, from http://www.nature.com/articles/s41586-021-03981-7 (Number: 7889 Publisher: Nature Publishing Group) doi: 10.1038/s41586-021-03981-7

Hausfather, Z., & Peters, G. P. (2020, January). Emissions – the 'business as usual' story is misleading. *Nature*, *577*(7792), 618–620. Retrieved 2022-05-17, from http://www.nature.com/articles/d41586-020-00177-3 (Bandiera_abtest: a Cg_type: Comment Number: 7792 Publisher: Nature Publishing Group Subject_term: Climate change, Climate sciences, Energy, Policy, Society) doi: 10.1038/d41586-020-00177-3

Haywood, J. M., Jones, A., Bellouin, N., & Stephenson, D. (2013, July). Asymmetric forcing from stratospheric aerosols impacts Sahelian rainfall. *Nature Clim Change*, *3*(7), 660–665. Retrieved 2022-01-19, from http://www.nature.com/articles/nclimate1857 (Bandiera_abtest: a Cg_type: Nature Research Journals Number: 7 Primary_atype: Research Publisher: Nature Publishing Group Subject_term: Atmospheric science;Climate sciences;Environmental social sciences Subject_term_id: atmospheric-science;climate-sciences;environmental-social-sciences) doi: 10.1038/nclimate1857

Heijmans, M. M. P. D., Magnusson, R. I., Lara, M. J., Frost, G. V., Myers-Smith, I. H., van Huissteden, J., … Limpens, J. (2022, January). Tundra vegetation change and impacts on permafrost. *Nat Rev Earth Environ*, *3*(1), 68–84. Retrieved 2022-07-18, from http://www.nature.com/articles/s43017-021-00233-0 (Number: 1 Publisher: Nature Publishing Group) doi: 10.1038/s43017-021-00233-0

Hobday, A. J., Alexander, L. V., Perkins, S. E., Smale, D. A., Straub, S. C., Oliver, E. C., … Wernberg, T. (2016, February). A hierarchical approach to defining marine heatwaves. *Progress in Oceanography*, *141*, 227–238. Retrieved 2021-04-26, from https://linkinghub.elsevier.com/retrieve/pii/S0079661116000057 doi: 10.1016/j.pocean.2015.12.014

Holbrook, N., Gupta, A., Oliver, E., Hobday, A., Benthuysen, J., Scannell, H., … Wernberg, T. (2020, July). Keeping pace with marine heatwaves. *Nature Reviews Earth & Environment*, *1*. doi: 10.1038/s43017-020-0068-4

Hueholt, D. (2022). *PAPER - Assessing Outcomes in Stratospheric Aerosol Injection Scenarios Shortly After Deployment.* Retrieved 2022-12-16, from https://osf.io/5a2zf/ (Publisher: OSF)

Hurrell, J. W., Holland, M. M., Gent, P. R., Ghan, S., Kay, J. E., Kushner, P. J., … Marshall, S. (2013, September). The Community Earth System Model: A Framework for Collaborative Research. *Bulletin of the American Meteorological Society*, *94*(9), 1339–1360. Retrieved 2022-08-08, from http://journals.ametsoc.org/view/journals/bams/94/9/bams-d-12-00121.1.xml (Publisher: American Meteorological Society Section: Bulletin of the American Meteorological Society) doi: 10.1175/BAMS-D-12-00121.1

Iles, C. E., & Hegerl, G. C. (2014, October). The global precipitation response to volcanic eruptions in the CMIP5 models. *Environ. Res. Lett.*, *9*(10), 104012. Retrieved 2022-08-03, from https://doi.org/10.1088/1748-9326/9/10/104012 (Publisher: IOP Publishing) doi: 10.1088/1748-9326/9/10/104012

IPCC. (2021). *Climate Change 2021: The Physical Science Basis. Contribution of Working Group14 I to the Sixth Assessment Report of the Intergovernmental Panel on Climate Change; Technical Summary* (Tech. Rep.). Geneva, Switzerland: Intergovernmental Panel on Climate Change.

Jones, A., Haywood, J. M., Alterskjær, K., Boucher, O., Cole, J. N. S., Curry, C. L., … Yoon, J.-H. (2013). The impact of abrupt suspension of solar radiation management (termination effect) in experiment G2 of the Geoengineering Model Intercomparison Project (GeoMIP). *Journal of Geophysical Research: Atmospheres*, *118*(17), 9743–9752. Retrieved 2022-08-15, from http://onlinelibrary.wiley.com/doi/abs/10.1002/jgrd.50762 (_eprint: https://agupubs.onlinelibrary.wiley.com/doi/pdf/10.1002/jgrd.50762) doi: 10.1002/jgrd.50762

Kang, S. M., Shin, Y., & Xie, S.-P. (2018, January). Extratropical forcing and tropical rainfall distribution: energetics framework and ocean Ekman advection. *npj*

Clim Atmos Sci, *1*(1), 1–10. Retrieved 2022-09-09, from http://www.nature.com/articles/s41612-017-0004-6 (Number: 1 Publisher: Nature Publishing Group) doi: 10.1038/s41612-017-0004-6

Kay, J. E., Deser, C., Phillips, A., Mai, A., Hannay, C., Strand, G., ... Vertenstein, M. (2015, August). The Community Earth System Model (CESM) Large Ensemble Project: A Community Resource for Studying Climate Change in the Presence of Internal Climate Variability. *Bulletin of the American Meteorological Society*, *96*(8), 1333–1349. Retrieved 2022-09-14, from http://journals.ametsoc.org/view/journals/bams/96/8/bams-d-13-00255.1.xml (Publisher: American Meteorological Society Section: Bulletin of the American Meteorological Society) doi: 10.1175/BAMS-D-13-00255.1

Keys, P. W., Barnes, E. A., Diffenbaugh, N. S., Hurrell, J. W., & Bell, C. M. (2022, October). Potential for perceived failure of stratospheric aerosol injection deployment. *Proceedings of the National Academy of Sciences*, *119*(40), e2210036119. Retrieved 2022-10-07, from http://www.pnas.org/doi/abs/10.1073/pnas.2210036119 (Publisher: Proceedings of the National Academy of Sciences) doi: 10.1073/pnas.2210036119

King, M. D., Howat, I. M., Candela, S. G., Noh, M. J., Jeong, S., Noël, B. P. Y., ... Negrete, A. (2020, August). Dynamic ice loss from the Greenland Ice Sheet driven by sustained glacier retreat. *Communications Earth & Environment*, *1*(1), 1–7. Retrieved 2021-04-26, from http://www.nature.com/articles/s43247-020-0001-2 (Number: 1 Publisher: Nature Publishing Group) doi: 10.1038/s43247-020-0001-2

Kirchmeier-Young, M. C., & Zhang, X. (2020, June). Human influence has intensified extreme precipitation in North America. *Proceedings of the National Academy of Sciences*, *117*(24), 13308–13313. Retrieved 2022-08-09, from http://www.pnas.org/doi/abs/10.1073/pnas.1921628117 (Publisher: Proceedings of the National Academy of Sciences) doi: 10.1073/pnas.1921628117

Kravitz, B., MacMartin, D. G., Mills, M. J., Richter, J. H., Tilmes, S., Lamarque, J.-F., ... Vitt, F. (2017). First Simulations of Designing Stratospheric Sulfate Aerosol Geoengineering to Meet Multiple Simultaneous Climate Objectives. *Journal of Geophysical Research: Atmospheres*, *122*(23), 12,616–12,634. Retrieved 2020-12-21, from http://agupubs.onlinelibrary.wiley.com/doi/abs/10.1002/2017JD026874 (_eprint: https://onlinelibrary.wiley.com/doi/pdf/10.1002/2017JD026874) doi: https://doi.org/10.1002/2017JD026874

Kravitz, B., Robock, A., Boucher, O., Schmidt, H., Taylor, K. E., Stenchikov, G., & Schulz, M. (2011). The Geoengineering Model Intercomparison Project (GeoMIP). *Atmospheric Science Letters*, *12*(2), 162–167. Retrieved 2022-08-15, from http://onlinelibrary.wiley.com/doi/abs/10.1002/asl.316 (_eprint: https://rmets.onlinelibrary.wiley.com/doi/pdf/10.1002/asl.316) doi: 10.1002/asl.316

Kulkarni, A., Gadgil, S., & Patwardhan, S. (2016). Monsoon variability, the 2015 Marathwada drought and rainfed agriculture. *Current Science*, *111*(7), 1182–1193.

Kwiatkowski, L., Cox, P., Halloran, P. R., Mumby, P. J., & Wiltshire, A. J. (2015, August). Coral bleaching under unconventional scenarios of climate warming and ocean acidification. *Nature Clim Change*, *5*(8), 777–781. Retrieved 2022-08-15, from http://www.nature.com/articles/nclimate2655 (Number: 8 Publisher: Nature Publishing Group) doi: 10.1038/nclimate2655

Laaidi, K., Zeghnoun, A., Dousset, B., Bretin, P., Vandentorren, S., Giraudet, E., & Beaudeau, P. (2012, February). The Impact of Heat Islands on Mortality in Paris during the August 2003 Heat Wave. *Environmental Health Perspectives*, *120*(2), 254–259. Retrieved 2022-05-18, from https://ehp.niehs.nih.gov/doi/full/10.1289/ehp.1103532 (Publisher:

Environmental Health Perspectives) doi: 10.1289/ehp.1103532
Lee, W., MacMartin, D., Visioni, D., & Kravitz, B. (2020, November). Expanding the design space of stratospheric aerosol geoengineering to include precipitation-based objectives and explore trade-offs. *Earth System Dynamics*, *11*(4), 1051–1072. Retrieved 2022-01-11, from https://esd.copernicus.org/articles/11/1051/2020/ (Publisher: Copernicus GmbH) doi: 10.5194/esd-11-1051-2020
Long, J. C. S., & Shepherd, J. G. (2014). The Strategic Value of Geoengineering Research. In B. Freedman (Ed.), *Global Environmental Change* (pp. 757–770). Dordrecht: Springer Netherlands. Retrieved 2022-08-16, from https://doi.org/10.1007/978-94-007-5784-4_24 doi: 10.1007/978-94-007-5784-4_24
MacMartin, D. G., & Kravitz, B. (2019, May). The Engineering of Climate Engineering. *Annu. Rev. Control Robot. Auton. Syst.*, *2*(1), 445–467. Retrieved 2021-09-28, from https://doi.org/10.1146/annurev-control-053018-023725 (Publisher: Annual Reviews) doi: 10.1146/annurev-control-053018-023725
MacMartin, D. G., Kravitz, B., Keith, D. W., & Jarvis, A. (2014, July). Dynamics of the coupled human–climate system resulting from closed-loop control of solar geoengineering. *Clim Dyn*, *43*(1), 243–258. Retrieved 2022-05-17, from https://doi.org/10.1007/s00382-013-1822-9 doi: 10.1007/s00382-013-1822-9
MacMartin, D. G., Kravitz, B., Tilmes, S., Richter, J. H., Mills, M. J., Lamarque, J.-F., ... Vitt, F. (2017). The Climate Response to Stratospheric Aerosol Geoengineering Can Be Tailored Using Multiple Injection Locations. *Journal of Geophysical Research: Atmospheres*, *122*(23), 12,574–12,590. Retrieved 2021-05-28, from http://agupubs.onlinelibrary.wiley.com/doi/abs/10.1002/2017JD026868 (_eprint: https://onlinelibrary.wiley.com/doi/pdf/10.1002/2017JD026868) doi: https://doi.org/10.1002/2017JD026868
MacMartin, D. G., Visioni, D., Kravitz, B., Richter, J., Felgenhauer, T., Lee, W. R., ... Sugiyama, M. (2022, August). Scenarios for modeling solar radiation modification. *Proceedings of the National Academy of Sciences*, *119*(33), e2202230119. Retrieved 2022-08-09, from http://www.pnas.org/doi/10.1073/pnas.2202230119 (Publisher: Proceedings of the National Academy of Sciences) doi: 10.1073/pnas.2202230119
Maher, N., Milinski, S., & Ludwig, R. (2021, April). Large ensemble climate model simulations: introduction, overview, and future prospects for utilising multiple types of large ensemble. *Earth System Dynamics*, *12*(2), 401–418. Retrieved 2022-05-19, from https://esd.copernicus.org/articles/12/401/2021/ (Publisher: Copernicus GmbH) doi: 10.5194/esd-12-401-2021
Massom, R. A., Scambos, T. A., Bennetts, L. G., Reid, P., Squire, V. A., & Stammerjohn, S. E. (2018, June). Antarctic ice shelf disintegration triggered by sea ice loss and ocean swell. *Nature*, *558*(7710), 383–389. Retrieved 2021-11-12, from http://www.nature.com/articles/s41586-018-0212-1 (Bandiera_abtest: a Cg_type: Nature Research Journals Number: 7710 Primary_atype: Research Publisher: Nature Publishing Group Subject_term: Cryospheric science;Physical oceanography Subject_term_id: cryospheric-science;physical-oceanography) doi: 10.1038/s41586-018-0212-1
Matthews, H. D., & Wynes, S. (2022, June). Current global efforts are insufficient to limit warming to 1.5°C. *Science*, *376*(6600), 1404–1409. Retrieved 2022-08-10, from http://www.science.org/doi/full/10.1126/science.abo3378 (Publisher: American Association for the Advancement of Science) doi: 10.1126/science.abo3378
McCusker, K. E., Battisti, D. S., & Bitz, C. M. (2015). Inability of stratospheric

sulfate aerosol injections to preserve the West Antarctic Ice Sheet. *Geophysical Research Letters*, *42*(12), 4989–4997. Retrieved 2022-08-15, from http://onlinelibrary.wiley.com/doi/abs/10.1002/2015GL064314 (_eprint: https://agupubs.onlinelibrary.wiley.com/doi/pdf/10.1002/2015GL064314) doi: 10.1002/2015GL064314

Melvin, A. M., Larsen, P., Boehlert, B., Neumann, J. E., Chinowsky, P., Espinet, X., … Marchenko, S. S. (2017, January). Climate change damages to Alaska public infrastructure and the economics of proactive adaptation. *Proceedings of the National Academy of Sciences*, *114*(2), E122–E131. Retrieved 2022-07-18, from https://www.pnas.org/doi/full/10.1073/pnas.1611056113 (Publisher: Proceedings of the National Academy of Sciences) doi: 10.1073/pnas.1611056113

MHIWG. (2022). *All about MHWs.* Retrieved 2022-05-19, from http://www.marineheatwaves.org/all-about-mhws.html

Mills, M., Visioni, D., & Richter, J. (2022). *CESM2-WACCM-SSP245 simulations [Dataset].* UCAR/NCAR - CISL - CDP. Retrieved 2022-12-16, from https://www.earthsystemgrid.org/dataset/ucar.cgd.cesm2.waccm6.ssp245.html (Type: dataset) doi: 10.26024/0CS0-EV98

Mills, M. J., Richter, J. H., Tilmes, S., Kravitz, B., MacMartin, D. G., Glanville, A. A., … Kinnison, D. E. (2017). Radiative and Chemical Response to Interactive Stratospheric Sulfate Aerosols in Fully Coupled CESM1(WACCM). *Journal of Geophysical Research: Atmospheres*, *122*(23), 13,061–13,078. Retrieved 2021-05-28, from http://agupubs.onlinelibrary.wiley.com/doi/abs/10.1002/2017JD027006 (_eprint: https://onlinelibrary.wiley.com/doi/pdf/10.1002/2017JD027006) doi: https://doi.org/10.1002/2017JD027006

Moreno-Chamarro, E., Marshall, J., & Delworth, T. L. (2019, December). Linking ITCZ Migrations to the AMOC and North Atlantic/Pacific SST Decadal Variability. *Journal of Climate*, *33*(3), 893–905. Retrieved 2021-11-05, from http://journals.ametsoc.org/view/journals/clim/33/3/jcli-d-19-0258.1.xml (Publisher: American Meteorological Society Section: Journal of Climate) doi: 10.1175/JCLI-D-19-0258.1

Morgenstern, O., Braesicke, P., Hurwitz, M. M., O'Connor, F. M., Bushell, A. C., Johnson, C. E., & Pyle, J. A. (2008). The World Avoided by the Montreal Protocol. *Geophysical Research Letters*, *35*(16). Retrieved 2021-11-18, from http://onlinelibrary.wiley.com/doi/abs/10.1029/2008GL034590 (_eprint: https://agupubs.onlinelibrary.wiley.com/doi/pdf/10.1029/2008GL034590) doi: 10.1029/2008GL034590

Moriyama, R., Sugiyama, M., Kurosawa, A., Masuda, K., Tsuzuki, K., & Ishimoto, Y. (2017, December). The cost of stratospheric climate engineering revisited. *Mitig Adapt Strateg Glob Change*, *22*(8), 1207–1228. Retrieved 2022-07-25, from https://doi.org/10.1007/s11027-016-9723-y doi: 10.1007/s11027-016-9723-y

NASEM. (2021). *Reflecting Sunlight: Recommendations for Solar Geoengineering Research and Research Governance* (Tech. Rep.). Washington, D.C.: National Academies of Science, Engineering, and Medicine.

NCAR. (2022). *Community Earth System Model v2 ARISE (CESM2 ARISE) - Registry of Open Data on AWS [Dataset].* Retrieved 2022-12-16, from https://registry.opendata.aws/ncar-cesm2-arise/

Nicholson, S. E. (2017). Climate and climatic variability of rainfall over eastern Africa. *Reviews of Geophysics*, *55*(3), 590–635. Retrieved 2022-06-22, from http://onlinelibrary.wiley.com/doi/abs/10.1002/2016RG000544 (_eprint: https://agupubs.onlinelibrary.wiley.com/doi/pdf/10.1002/2016RG000544)

doi: 10.1002/2016RG000544
NSIDC. (2020). *Data: Terminology | National Snow and Ice Data Center.* Retrieved 2022-05-19, from https://nsidc.org/cryosphere/seaice/data/terminology.html
Oliver, E. (2022, May). *Marine Heatwaves detection code.* Retrieved 2022-05-19, from https://github.com/ecjoliver/marineHeatWaves (original-date: 2015-04-28T07:33:04Z)
Panetta, A. M., Stanton, M. L., & Harte, J. (2018, February). Climate warming drives local extinction: Evidence from observation and experimentation. *Science Advances*, *4*(2), eaaq1819. Retrieved 2022-08-12, from http://www.science.org/doi/10.1126/sciadv.aaq1819 (Publisher: American Association for the Advancement of Science) doi: 10.1126/sciadv.aaq1819
Parkinson, C. L. (2019, July). A 40-y record reveals gradual Antarctic sea ice increases followed by decreases at rates far exceeding the rates seen in the Arctic. *Proceedings of the National Academy of Sciences*, *116*(29), 14414–14423. Retrieved 2022-05-17, from https://www.pnas.org/doi/10.1073/pnas.1906556116 (Publisher: Proceedings of the National Academy of Sciences) doi: 10.1073/pnas.1906556116
Pearman, O., & Cravens, A. E. (2022, February). Institutional barriers to actionable science: Perspectives from decision support tool creators. *Environmental Science & Policy*, *128*, 317–325. Retrieved 2022-08-08, from https://www.sciencedirect.com/science/article/pii/S1462901121003592 doi: 10.1016/j.envsci.2021.12.004
Pinto, I., Jack, C., Lennard, C., Tilmes, S., & Odoulami, R. C. (2020). Africa's Climate Response to Solar Radiation Management With Stratospheric Aerosol. *Geophysical Research Letters*, *47*(2), e2019GL086047. Retrieved 2021-11-02, from http://onlinelibrary.wiley.com/doi/abs/10.1029/2019GL086047 (_eprint: https://agupubs.onlinelibrary.wiley.com/doi/pdf/10.1029/2019GL086047) doi: 10.1029/2019GL086047
Quaglia, I., Timmreck, C., Niemeier, U., Visioni, D., Pitari, G., Brodowsky, C., ... Sukhodolov, T. (2023, January). Interactive stratospheric aerosol models' response to different amounts and altitudes of SO2 injection during the 1991 Pinatubo eruption. *Atmospheric Chemistry and Physics*, *23*(2), 921–948. Retrieved 2023-03-10, from https://acp.copernicus.org/articles/23/921/2023/ (Publisher: Copernicus GmbH) doi: 10.5194/acp-23-921-2023
Rajaud, A., & Noblet-Ducoudré, N. d. (2017, October). Tropical semi-arid regions expanding over temperate latitudes under climate change. *Climatic Change*, *144*(4), 703–719. Retrieved 2022-03-21, from https://doi.org/10.1007/s10584-017-2052-7 doi: 10.1007/s10584-017-2052-7
Rasch, P. J., Tilmes, S., Turco, R. P., Robock, A., Oman, L., Chen, C.-C. J., ... Garcia, R. R. (2008, November). An overview of geoengineering of climate using stratospheric sulphate aerosols. *Philosophical Transactions of the Royal Society A: Mathematical, Physical and Engineering Sciences*, *366*(1882), 4007–4037. Retrieved 2022-11-16, from https://royalsocietypublishing.org/doi/full/10.1098/rsta.2008.0131 (Publisher: Royal Society) doi: 10.1098/rsta.2008.0131
Rathi, S. K., Sodani, P. R., & Joshi, S. (2021, June). Summer Temperature and All-cause Mortality from 2006 to 2015 for Smart City Jaipur, India. *Journal of Health Management*, *23*(2), 294–301. Retrieved 2022-05-18, from https://doi.org/10.1177/09720634211011693 (Publisher: SAGE Publications India) doi: 10.1177/09720634211011693
Riahi, K., van Vuuren, D. P., Kriegler, E., Edmonds, J., O'Neill, B. C., Fujimori, S., ... Tavoni, M. (2017, January). The Shared Socioeconomic Pathways and their energy, land use, and greenhouse gas emissions implications: An

overview. *Global Environmental Change*, *42*, 153–168. Retrieved 2020-12-04, from http://www.sciencedirect.com/science/article/pii/S0959378016300681 doi: 10.1016/j.gloenvcha.2016.05.009

Richter, H., Jadwiga, Tilmes, S., Glanville, A., Kravitz, B., MacMartin, D. G., Mills, M. J., … Lamarque, J.-F. (2018). Stratospheric Response in the First Geoengineering Simulation Meeting Multiple Surface Climate Objectives. *Journal of Geophysical Research: Atmospheres*, *123*(11), 5762–5782. Retrieved 2022-08-08, from http://onlinelibrary.wiley.com/doi/abs/10.1029/2018JD028285 (_eprint: https://agupubs.onlinelibrary.wiley.com/doi/pdf/10.1029/2018JD028285) doi: 10.1029/2018JD028285

Richter, J. H. (2022). *Assessing Responses and Impacts of Solar climate intervention on the Earth system with stratospheric aerosol injection simulations (ARISE-SAI-1.5) [Dataset].* UCAR/NCAR - CISL - CDP. Retrieved 2022-12-16, from https://www.earthsystemgrid.org/dataset/id/29c8320f-c525-4cd2-8014-361eecec3907.html (Type: dataset) doi: 10.5065/9KCN-9Y79

Richter, J. H., Tilmes, S., Mills, M. J., Tribbia, J. J., Kravitz, B., MacMartin, D. G., … Lamarque, J.-F. (2017). Stratospheric Dynamical Response and Ozone Feedbacks in the Presence of SO2 Injections. *Journal of Geophysical Research: Atmospheres*, *122*(23), 12,557–12,573. Retrieved 2021-05-28, from http://agupubs.onlinelibrary.wiley.com/doi/abs/10.1002/2017JD026912 (_eprint: https://onlinelibrary.wiley.com/doi/pdf/10.1002/2017JD026912) doi: https://doi.org/10.1002/2017JD026912

Richter, J. H., Visioni, D., MacMartin, D. G., Bailey, D. A., Rosenbloom, N., Dobbins, B., … Lamarque, J.-F. (2022, November). Assessing Responses and Impacts of Solar climate intervention on the Earth system with stratospheric aerosol injection (ARISE-SAI): protocol and initial results from the first simulations. *Geoscientific Model Development*, *15*(22), 8221–8243. Retrieved 2022-11-23, from https://gmd.copernicus.org/articles/15/8221/2022/ (Publisher: Copernicus GmbH) doi: 10.5194/gmd-15-8221-2022

Robock, A., Oman, L., & Stenchikov, G. L. (2008). Regional climate responses to geoengineering with tropical and Arctic SO2 injections. *Journal of Geophysical Research: Atmospheres*, *113*(D16). Retrieved 2022-07-15, from http://onlinelibrary.wiley.com/doi/abs/10.1029/2008JD010050 (_eprint: https://agupubs.onlinelibrary.wiley.com/doi/pdf/10.1029/2008JD010050) doi: 10.1029/2008JD010050

Rugenstein, M. A. A., Gregory, J. M., Schaller, N., Sedláček, J., & Knutti, R. (2016, August). Multiannual Ocean–Atmosphere Adjustments to Radiative Forcing. *Journal of Climate*, *29*(15), 5643–5659. Retrieved 2022-06-14, from http://journals.ametsoc.org/view/journals/clim/29/15/jcli-d-16-0312.1.xml (Publisher: American Meteorological Society Section: Journal of Climate) doi: 10.1175/JCLI-D-16-0312.1

Shearer, C. (2012). The Social Construction of Alaska Native Vulnerability to Climate Change. *Race, Gender & Class*, *19*(1/2), 61–79. Retrieved 2022-07-20, from https://www.jstor.org/stable/43496860 (Publisher: Jean Ait Belkhir, Race, Gender & Class Journal)

Sherwood, S. C., Bony, S., Boucher, O., Bretherton, C., Forster, P. M., Gregory, J. M., & Stevens, B. (2015, February). Adjustments in the Forcing-Feedback Framework for Understanding Climate Change. *Bulletin of the American Meteorological Society*, *96*(2), 217–228. Retrieved 2022-06-14, from http://journals.ametsoc.org/view/journals/bams/96/2/bams-d-13-00167.1.xml (Publisher: American Meteorological Society Section: Bulletin of the American Meteorological Society) doi: 10.1175/BAMS-D-13-00167.1

Sillmann, J., & Roeckner, E. (2008, January). Indices for extreme events in projections of anthropogenic climate change. *Climatic Change*, *86*(1), 83–104. Retrieved 2022-05-18, from https://doi.org/10.1007/s10584-007-9308-6 doi: 10.1007/s10584-007-9308-6

Simpson, I. R., Tilmes, S., Richter, J. H., Kravitz, B., MacMartin, D. G., Mills, M. J., ... Pendergrass, A. G. (2019). The Regional Hydroclimate Response to Stratospheric Sulfate Geoengineering and the Role of Stratospheric Heating. *Journal of Geophysical Research: Atmospheres*, *124*(23), 12587–12616. Retrieved 2020-12-22, from http://agupubs.onlinelibrary.wiley.com/doi/abs/10.1029/2019JD031093 (_eprint: https://onlinelibrary.wiley.com/doi/pdf/10.1029/2019JD031093) doi: https://doi.org/10.1029/2019JD031093

Smith, K. E., Burrows, M. T., Hobday, A. J., Sen Gupta, A., Moore, P. J., Thomsen, M., ... Smale, D. A. (2021, October). Socioeconomic impacts of marine heatwaves: Global issues and opportunities. *Science*, *374*(6566), eabj3593. Retrieved 2022-08-09, from http://www.science.org/doi/full/10.1126/science.abj3593 (Publisher: American Association for the Advancement of Science) doi: 10.1126/science.abj3593

Smith, W., Bhattarai, U., Bingaman, D. C., Mace, J. L., & Rice, C. V. (2022, March). Review of possible very high-altitude platforms for stratospheric aerosol injection. *Environ. Res. Commun.*, *4*(3), 031002. Retrieved 2022-07-25, from https://doi.org/10.1088/2515-7620/ac4f5d (Publisher: IOP Publishing) doi: 10.1088/2515-7620/ac4f5d

Sniderman, J. M. K., Brown, J. R., Woodhead, J. D., King, A. D., Gillett, N. P., Tokarska, K. B., ... Meinshausen, M. (2019, March). Southern Hemisphere subtropical drying as a transient response to warming. *Nat. Clim. Chang.*, *9*(3), 232–236. Retrieved 2022-02-18, from http://www.nature.com/articles/s41558-019-0397-9 (Number: 3 Publisher: Nature Publishing Group) doi: 10.1038/s41558-019-0397-9

Stroeve, J. C., Serreze, M. C., Holland, M. M., Kay, J. E., Malanik, J., & Barrett, A. P. (2012, February). The Arctic's rapidly shrinking sea ice cover: a research synthesis. *Climatic Change*, *110*(3), 1005–1027. Retrieved 2022-05-17, from https://doi.org/10.1007/s10584-011-0101-1 doi: 10.1007/s10584-011-0101-1

Swann, A. L., Fung, I. Y., Levis, S., Bonan, G. B., & Doney, S. C. (2010, January). Changes in Arctic vegetation amplify high-latitude warming through the greenhouse effect. *Proceedings of the National Academy of Sciences*, *107*(4), 1295–1300. Retrieved 2022-07-18, from https://www.pnas.org/doi/abs/10.1073/pnas.0913846107 (Publisher: Proceedings of the National Academy of Sciences) doi: 10.1073/pnas.0913846107

Talberg, A., Thomas, S., Christoff, P., & Karoly, D. (2018, July). How geoengineering scenarios frame assumptions and create expectations. *Sustain Sci*, *13*(4), 1093–1104. Retrieved 2022-08-05, from https://doi.org/10.1007/s11625-018-0527-8 doi: 10.1007/s11625-018-0527-8

Tebaldi, C., Dorheim, K., Wehner, M., & Leung, R. (2021, December). Extreme metrics from large ensembles: investigating the effects of ensemble size on their estimates. *Earth System Dynamics*, *12*(4), 1427–1501. Retrieved 2022-08-09, from https://esd.copernicus.org/articles/12/1427/2021/ (Publisher: Copernicus GmbH) doi: 10.5194/esd-12-1427-2021

The Royal Society. (2009). *Geoengineering the Climate* (Tech. Rep.). London, U.K.: The Royal Society.

Tilmes, S., Garcia, R. R., Kinnison, D. E., Gettelman, A., & Rasch, P. J. (2009, June). Impact of geoengineered aerosols on the troposphere and stratosphere. *Journal of Geophysical Research: Atmospheres*, *114*(D12). Retrieved 2021-05-19, from http://agupubs.onlinelibrary.wiley.com/doi/10.1029/2008JD011420 (Publisher: John Wiley & Sons, Ltd) doi:

10.1029/2008JD011420
Tilmes, S., & Richter, J. H. (2018). *Stratospheric Aerosol Geoengineering Large Ensemble [Dataset].* UCAR/NCAR Earth System Grid. Retrieved 2022-12-16, from http://www.cesm.ucar.edu/community-projects/GLENS (Type: dataset) doi: 10.5065/D6JH3JXX

Tilmes, S., Richter, J. H., Kravitz, B., MacMartin, D. G., Mills, M. J., Simpson, I. R., … Ghosh, S. (2018, November). CESM1(WACCM) Stratospheric Aerosol Geoengineering Large Ensemble Project. *Bulletin of the American Meteorological Society*, *99*(11), 2361–2371. Retrieved 2021-07-06, from http://journals.ametsoc.org/view/journals/bams/99/11/bams-d-17-0267.1.xml (Publisher: American Meteorological Society Section: Bulletin of the American Meteorological Society) doi: 10.1175/BAMS-D-17-0267.1

Tilmes, S., Richter, J. H., Mills, M. J., Kravitz, B., MacMartin, D. G., Garcia, R. R., … Vitt, F. (2018). Effects of Different Stratospheric SO2 Injection Altitudes on Stratospheric Chemistry and Dynamics. *Journal of Geophysical Research: Atmospheres*, *123*(9), 4654–4673. Retrieved 2022-05-18, from http://onlinelibrary.wiley.com/doi/abs/10.1002/2017JD028146 (_eprint: https://agupubs.onlinelibrary.wiley.com/doi/pdf/10.1002/2017JD028146) doi: 10.1002/2017JD028146

Tilmes, S., Richter, J. H., Mills, M. J., Kravitz, B., MacMartin, D. G., Vitt, F., … Lamarque, J.-F. (2017). Sensitivity of Aerosol Distribution and Climate Response to Stratospheric SO2 Injection Locations. *Journal of Geophysical Research: Atmospheres*, *122*(23), 12,591–12,615. Retrieved 2021-05-28, from http://agupubs.onlinelibrary.wiley.com/doi/abs/10.1002/2017JD026888 (_eprint: https://onlinelibrary.wiley.com/doi/pdf/10.1002/2017JD026888) doi: https://doi.org/10.1002/2017JD026888

Timmreck, C. (2012). Modeling the climatic effects of large explosive volcanic eruptions. *WIREs Climate Change*, *3*(6), 545–564. Retrieved 2020-11-09, from https://onlinelibrary.wiley.com/doi/abs/10.1002/wcc.192 (_eprint: https://onlinelibrary.wiley.com/doi/pdf/10.1002/wcc.192) doi: https://doi.org/10.1002/wcc.192

Tomkins, L. M., Yuter, S. E., Miller, M. A., & Allen, L. R. (2022, September). Image muting of mixed precipitation to improve identification of regions of heavy snow in radar data. *Atmospheric Measurement Techniques*, *15*(18), 5515–5525. Retrieved 2022-09-28, from https://amt.copernicus.org/articles/15/5515/2022/ (Publisher: Copernicus GmbH) doi: 10.5194/amt-15-5515-2022

Trisos, C. H., Amatulli, G., Gurevitch, J., Robock, A., Xia, L., & Zambri, B. (2018, March). Potentially dangerous consequences for biodiversity of solar geoengineering implementation and termination. *Nat Ecol Evol*, *2*(3), 475–482. Retrieved 2022-08-15, from http://www.nature.com/articles/s41559-017-0431-0 (Number: 3 Publisher: Nature Publishing Group) doi: 10.1038/s41559-017-0431-0

Tye, M. R., Dagon, K., Molina, M. J., Richter, J. H., Visioni, D., Kravitz, B., & Tilmes, S. (2022, August). Indices of extremes: geographic patterns of change in extremes and associated vegetation impacts under climate intervention. *Earth System Dynamics*, *13*(3), 1233–1257. Retrieved 2022-08-29, from https://esd.copernicus.org/articles/13/1233/2022/ (Publisher: Copernicus GmbH) doi: 10.5194/esd-13-1233-2022

Undorf, S., Polson, D., Bollasina, M. A., Ming, Y., Schurer, A., & Hegerl, G. C. (2018). Detectable Impact of Local and Remote Anthropogenic Aerosols on the 20th Century Changes of West African and South Asian Monsoon Precipitation. *Journal of Geophysical Research: Atmospheres*, *123*(10), 4871–4889. Retrieved 2022-09-09, from http://onlinelibrary.wiley.com/doi/abs/10.1029/2017JD027711 (_eprint:

https://agupubs.onlinelibrary.wiley.com/doi/pdf/10.1029/2017JD027711) doi: 10.1029/2017JD027711

van Oldenborgh, G. J., Collins, M., Arblaster, J., Christensen, J. H., Marotzke, J., Power, S. B., ... Zhou, T. (2013). Annex I: Atlas of Global and Regional Climate Projections. In T. F. Stocker et al. (Eds.), (pp. 1311–1393). Cambridge, United Kingdom: Cambridge University Press. Retrieved 2022-05-19, from `https://www.ipcc.ch/report/ar5/wg1/` (Num Pages: 84)

van Vuuren, D. P., Edmonds, J., Kainuma, M., Riahi, K., Thomson, A., Hibbard, K., ... Rose, S. K. (2011, August). The representative concentration pathways: an overview. *Climatic Change*, *109*(1), 5. Retrieved 2022-07-25, from `https://doi.org/10.1007/s10584-011-0148-z` doi: 10.1007/s10584-011-0148-z

Visioni, D., MacMartin, D. G., & Kravitz, B. (2021). Is Turning Down the Sun a Good Proxy for Stratospheric Sulfate Geoengineering? *Journal of Geophysical Research: Atmospheres*, *126*(5), e2020JD033952. Retrieved 2022-05-13, from `http://onlinelibrary.wiley.com/doi/abs/10.1029/2020JD033952` (_eprint: https://agupubs.onlinelibrary.wiley.com/doi/pdf/10.1029/2020JD033952) doi: 10.1029/2020JD033952

Visioni, D., MacMartin, D. G., Kravitz, B., Richter, J. H., Tilmes, S., & Mills, M. J. (2020). Seasonally Modulated Stratospheric Aerosol Geoengineering Alters the Climate Outcomes. *Geophysical Research Letters*, *47*(12), e2020GL088337. Retrieved 2023-03-10, from `https://onlinelibrary.wiley.com/doi/abs/10.1029/2020GL088337` (_eprint: https://onlinelibrary.wiley.com/doi/pdf/10.1029/2020GL088337) doi: 10.1029/2020GL088337

Wainwright, C. M., Finney, D. L., Kilavi, M., Black, E., & Marsham, J. H. (2021). Extreme rainfall in East Africa, October 2019–January 2020 and context under future climate change. *Weather*, *76*(1), 26–31. Retrieved 2022-06-22, from `http://onlinelibrary.wiley.com/doi/abs/10.1002/wea.3824` (_eprint: https://rmets.onlinelibrary.wiley.com/doi/pdf/10.1002/wea.3824) doi: 10.1002/wea.3824

Zhang, X., Alexander, L., Hegerl, G. C., Jones, P., Tank, A. K., Peterson, T. C., ... Zwiers, F. W. (2011). Indices for monitoring changes in extremes based on daily temperature and precipitation data. *WIREs Climate Change*, *2*(6), 851–870. Retrieved 2022-05-18, from `https://onlinelibrary.wiley.com/doi/abs/10.1002/wcc.147` (_eprint: https://onlinelibrary.wiley.com/doi/pdf/10.1002/wcc.147) doi: 10.1002/wcc.147

Zhang, Y., MacMartin, D. G., Visioni, D., & Kravitz, B. (2022, January). How large is the design space for stratospheric aerosol geoengineering? *Earth System Dynamics*, *13*(1), 201–217. Retrieved 2022-02-08, from `https://esd.copernicus.org/articles/13/201/2022/` (Publisher: Copernicus GmbH) doi: 10.5194/esd-13-201-2022